4-06-68-1 • MARCH 1968

4-06-68-1

LOW SOLAR ABSORPTANCE AND EMITTANCE SURFACES UTILIZING VACUUM DEPOSITED TECHNIQUES

S. A. GREENBERG

D. A. VANCE

LOW SOLAR ABSORPTANCE AND EMITTANCE SURFACES UTILIZING VACUUM DEPOSITED TECHNIQUES

4-06-68-1 March 1968

Contract No. NAS 2-3063

Final Report for Period
1 June 1967 to March 25, 1968

Prepared for
NASA
Ames Research Center
Moffett Field, Calif.

LOCKHEED PALO ALTO RESEARCH LABORATORY
LOCKHEED MISSILES & SPACE COMPANY
A GROUP DIVISION OF LOCKHEED AIRCRAFT CORPORATION

FOREWORD

This report was prepared by the Thermophysics Section of the Aerospace Sciences Laboratory, Lockheed Missiles & Space Company for NASA – Ames Research Center, Moffett Field, California, as the final report under contract NAS 2-3063. The work described was performed during the period 1 June 1967 to 25 March 1968.

ACKNOWLEDGMENTS

The authors wish to acknowledge the contributions of members of the Thermophysics Section of the LMSC Aerospace Sciences Laboratory. Dr. M. McCargo conducted the proton radiation tests. Hemispherical emittance measurements were made by G. Bell and measurements of spectral reflectance were made by S. Handlin and A. Funai.

The analysis of the optical properties of dielectric-metal systems was made by C. K. Liu and R. P. Caren.

The work was performed under the cognizance of Mr. Elmer Streed, Technical Monitor of NASA-Ames Research Center.

SUMMARY

This program is a continuation of the work as reported in Ref. 1, which is devoted to investigations of the techniques and materials for finishing spacecraft structural surfaces with stable, reproducible thermal control materials. Various coating systems, prepared by vacuum physical vapor deposition, were evaluated in terms of optical characteristics. Basic system parameters were deposition rate, film thickness, substrate material and finish. Coating systems selected for study were, (1) quartz substrates with second surface silver for low α_s, (2) polished aluminum alloy substrate with silver overcoated with silica for α_s/ϵ of 1.0 and low α_s, and (3) mill-finish aluminum alloy with silver and alumina overcoat for low ϵ.

The continuation of this work is a further investigation of vacuum deposited optical films with emphasis on the optical characterization of silver films and silver films with dielectric overlays. Stability of these films under conditions of high temperature and proton and ultraviolet radiation were studied.

The stability of second surface silver reflectors with fused silica substrates, OSR's (Optical Solar Reflector), under conditions of radiation of 2 keV protons with an integrated exposure of 5×10^{17} p/cm^2 was excellent. No degradation occurred on exposure at substrate temperatures up to 700 °K. Less than 1% decrease in solar transmittance of the fused silica resulted upon exposure to 500 equivalent sun-hours ultraviolet at 700 °K.

The total hemispherical emittance of the OSR was measured over the range of 400 °K to 800 °K. The transmittance as a function of thickness of silver films was investigated. An analytical and experimental study of thin (200 Å to 1000 Å) dielectric coatings upon vacuum deposited silver was made. Measurements of total hemispherical, normal and angular emittance were performed.

CONTENTS

ILLUSTRATIONS

TABLES

NOMENCLATURE

$A_S = A_B$	sample and receiver frontal area
a_b	blackbody absorptance
a'_s	sample absorptance for blackbody radiation at T_B and sample at T_S
a''_s	sample absorptance for blackbody radiation at T_B and sample at 80°K
ESH	equivalent sun-hr
F_{BS}	blackbody to sample
F_{SB}	sample to blackbody view factor
k	oxtinction coefficient
n	index of refraction
OSR	optical solar reflector
Q_C	calibration power input
Q_L	heat flux to blackbody thermal links
T_B	blackbody receiver temperature
T_S	sample temperature
Y_C	blackbody radiation exchange with wall during calibration run
Y_S	blackbody radiation exchange with wall during sample run
α_s	solar absorptance
ϵ_b	blackbody emittance at T_B
ϵ_s	sample emittance at T_S
ϵ_H	total hemispherical emittance
ϵ_N	normal emittance
θ	reflectance angle ($\theta = 0$, normal reflectance)
ρ_H	hemispherical reflectance
ρ_N	normal reflectance
σ	Stefan-Boltzmann's Constant

Section 1
INTRODUCTION

The initial work performed on contract NAS 2-3063 (Ref. 1), for NASA – Ames Research Center, was concerned with an investigation of techniques and materials for finishing spacecraft structural surfaces with stable, reproducible thermal control materials.

Various coating systems were prepared by vacuum physical vapor deposition and evaluated in terms of optical characteristics. Basic system parameters studied were deposition rate, film thickness, substrate material, and finish. Coating systems of interest were those with low solar absorptance α_s, low infrared emittance ϵ and ratios of absorptance to emittance α_s/ϵ varying from 2.0 to 0.07. Optical measurements were made of specimens before and after ultraviolet irradiation, with substrates at 294 °K and 533 °K during irradiation. Coating systems were selected to satisfy practical engineering requirements. These systems were, (1) quartz substrates with second surface silver for low α_s, (2) polished aluminum alloy substrate with silver overcoated with silica for α_s/ϵ of 1.0 and low α_s, and (3) mill-finish aluminum alloy with silver and alumina overcoat for low ϵ.

System (1) showed no change in optical characteristics when irradiated. System (2) and (3) showed no significant change in absorptance or emittance when subjected to 2000 ESH (equivalent sun-hours) at 294°K. Exposure to 2000 ESH at 533 °K resulted in a change in the solar absorptance of one system. This change was ascribed to diffusion and structure change.

The continuation of the work is concerned with the optical characterization of vacuum deposited silver and dielectric films and the investigation of their stability under conditions of high temperature and proton and ultraviolet radiation.

- Coating techniques and material characteristics were experimentally determined to provide a minimum value of solar absorptance.
- The stability of the spectral reflectance (0.3 to 1.8μ) of the coating system was experimentally determined for the following vacuum exposures:
  (1) 2 keV protons with an integrated exposure of 1×10^{16} p/cm^2, 1×10^{17} p/cm^2 and 5×10^{17} p/cm^2 at specimen temperatures of 400 °K, 530 °K and 700 °K. The following grades and sources of fused silica were tested: Suprasil II, Spectrasil B, Corning 7940 (Industrial), Corning 7940 (UV grade) and G.E. 151.
  (2) 500 ultraviolet solar radiation equivalent sun-hour exposure at 700 °K, using specimen materials as in (1).
- The total hemispherical emittance of a nominal (0.007-in.) thick fused silica surface with a vacuum deposited silver second surface was measured over the temperature range of 400 ° to 800 °K.
- The adhesion of the vacuum deposited silver to the fused silica was determined before and after exposure of each specimen using a Scotch tape test.

- An analytical and experimental study of the influence of thin (200 to 1000 Å) dielectric coatings upon the total hemispherical emittance of a vacuum deposited silver surface was performed.
  - An analytical relationship between the dielectric over-coating properties (optical thickness and complex refractive index) and the total hemispherical emittance was established.
  - Vacuum deposited silver with a minimum total hemispherical emittance was prepared on quartz and stainless steel substrates. Vacuum deposited aluminum oxide overcoatings with a minimum of three thicknesses in the range of 200 Å to 1000 Å were prepared. The total hemispherical emittance was measured for each thickness as a function of temperature over the range of 300 °K to 800 °K.
  - Total normal and angular emittance or reflectance measurements were performed at one temperature to verify the theory. Three thicknesses of alumina in the range of 200 to 1000 Å was tested.

Section 2
TECHNICAL PROGRAM

2.1 GENERAL

An investigation was made of silver films as first and second surface reflectors. The program was concerned with the definition of the processing parameters requisite to the specification of optical coating systems with low solar absorptance and both high emittance and minimum emittance which have application as thermal control surfaces for spacecraft in the near solar space environment. On the basis of the proposed mission environment, it was necessary to establish the stability of these coating systems under conditions of high temperature (to 700 °K), proton radiation (from 1×10^{16} to 5×10^{17} p/cm^2) and to uv radiation.

2.2 OBJECTIVES

The specific objectives of the program were:

- Investigate the transmittance versus thickness of vacuum deposited silver films.
  - The theoretical basis for an analytical relationship between the transmittance and the optical constants of silver were to be established from the literature and/or by derivation.
  - An experimental study of the correlation between spectral transmittance and silver film preparation parameters. Parameters studied were deposition rate and thickness.
  - Verification of the technique was demonstrated with three types of substrate materials, i.e., quartz, Mylar, sapphire.
- Investigation of the preparation, optical properties, and stability of second surface fused silica reflector coating system to attain low solar absorption and low ratio of solar absorptance to infrared emmitance.

2.3 THIN FILM DEPOSITION

The characteristics and techniques for the deposition of silver films and thin dielectric films of aluminum oxide overlay were studied. Definition of these techniques was made in order to establish reproducible and specified processes. In order to so establish process parameters, a correlation was made between the spectral transmission of the silver film and the deposition parameters, using fused silica, sapphire and Mylar substrates. In particular, the deposition parameters were determined for minimum solar absorptance. The principal deposition parameters were substrate preparation, deposition rate and film thickness.

The two coating systems studies were:

- OSR (optical solar reflector) which is a second surface mirror of silver on a fused silica substrate for low solar absorptance and a low ratio of solar absorptance to infrared emittance.
- Alumina overcoated silver for low solar absorptance and minimum emittance. The second system was studied for a range of dielectric thicknesses from 200 Å to 1000 Å.

2.4 ENVIRONMENTAL TESTS AND OPTICAL MEASUREMENTS

The optical characteristics of the silver and silver-dielectric systems were studied in three parts

2.4.1 Silver Films

The transmittance of vacuum deposited silver was measured for various film thicknesses and with changes in deposition parameters. Relationship between the transmittance and the optical constants were analytically determined.

2.4.2 OSR (Optical Solar Reflector)

The spectral reflectance in the range of 0.3 to 1.8μ was measured before and after radiation and heating in a vacuum environment.

The exposure conditions for proton, ultraviolet, and elevated temperature were as previously indicated (Section 2.2).

2.4.3 Dielectric-Metal Reflector

The relationship of varying film thicknesses of alumina, in the range of 200 to 1000 Å, overcoated on silver films to the total hemispherical emittance was established. Normal and angular emittance was also measured. The tasks performed were:

- Determination of the anlytical relationship between the optical properties of the dielectric overlay and the total hemispherical emittance.
- Measurement of the total hemispherical emittance for thin alumina films of three thicknesses in the range of 200 Å to 1000 Å. These films were overcoated on silver films which were deposited on quartz and stainless steel substrates. Emittance was measured for each thickness in the range of 300 °K to 800 °K.
- Measurement of total normal and angular emittance at one temperature

2.4.4 Mechanical Tests

Tests were performed to determine the adhesion and stability of the vacuum deposited films under consideration. The adhesion of the vacuum deposited silver to fused silica for the OSR system was determined by a scotch tape test.

2.5 THEORETICAL CONSIDERATIONS

2.5.1 Theory of Transmittance of Silver Film

The theoretical basis for an analytical relationship between the transmittance and reflectance and the optical constants of silver films on transparent substrates has

As shown in Section 6.7, the transmittance can be expressed as

$$T = \frac{16\, n_o (n_1^2 + k_1^2)^2 \exp\left(-\frac{4\pi k_1 d_1}{\lambda}\right)}{[(n_1 + 1)^2 + k_1^2][(n_o + n_1)^2 + k_1^2]}$$

where the index of the transparent substrate is n_o, and the thickness of the metal film is such that the effects of multiple reflections are suppressed. In the case of silver films this requirement imposes a lower limit of 300–400 Å on the thickness.

2.5.2 Emittance Theory

Francis and Love (Ref. 3) have analyzed the emittance characteristics of a metal-dielectric coating system, with the restriction, however that the optical thickness of the dielectric is greater than one wavelength.

Their results can be expressed in the form of an effective emittance, which accounts for reflection at the dielectric-air interface.

$$\epsilon_{eff}(\mu') = \frac{C_2\,[\rho_{1\nu}(\mu) \exp^{-2\, t_o/\mu} - 1]}{n^2 I_{bb\nu}(T)}$$

where

$$C_2 = \frac{n_d^2 I_{bb\nu}(T)\,[\rho_{2\nu}(\theta',\theta) - 1]}{1 - \rho_{2\nu}(\theta',\theta)\rho_{1\nu}(\mu) \exp^{-2\, t_o/\mu}}$$

and

n = refractive index ratio of dielectric to air

n_d = refractive index of dielectric

t_o = optical thickness of dielectric

been treated extensively in the literature (Ref. 2). For the case of normal incidence, the relationships may be expressed in the following form:

$$R = \frac{A \cosh \alpha + B \sinh \alpha - C \cos \zeta + D \sin \zeta}{E \cosh \alpha + F \sinh \alpha - G \cos \zeta + H \sin \zeta}$$

$$T = \frac{8\, n_o (n_1^2 + k_1^2)}{E \cosh \alpha + F \sinh \alpha - G \cos \zeta + H \sin \zeta}$$

where

$$\alpha = \frac{4\pi k d}{\lambda} \quad , \quad \zeta = \frac{4\pi n d}{\lambda}$$

and

$$A = (n^2 + h^2 + 1)(n^2 + k^2 + n_o^2) - 4n^2 n$$

$$B = 2n[n_o(n^2 + k^2 + 1) - (n^2 + k^2 + n_o^2]$$

$$C = (n^2 + k^2 - 1)(n^2 + k^2 - n_o^2) + 4k^2 n_o$$

$$D = 2k[n_o(n^2 + k^2 - 1) - (n^2 + k^2 - n_o^2)]$$

$$E = (n^2 + k^2 + 1)(n^2 + k^2 + n_o^2) + 4n^2 n_o$$

$$F = 2n[n_o(n^2 + k^2 + 1) + (n^2 + k^2 + n_o^2)]$$

$$G = (n^2 + k^2 - 1)(n^2 + k^2 - n_o^2) - 4k^2 n_o$$

$$H = 2k[n_o(n^2 + k^2 - 1) + (n^2 + k^2 - n_o^2)]$$

In these expressions the refractive index of the medium of incidence is assumed to be unity.

μ = $\cos \theta$

$\rho_{2\nu}(\theta', \theta)$ = directional reflectance at dielectric air interface

$\rho_{1\nu}(\mu)$ = directional reflectance of metal

$I_{bb\nu}(T)$ = monochromatic intensity of a blackbody at temperature T.

μ' = $[1 - n^2(1 - \mu^2)]^{1/2}$

The ratio of the angular emittance ϵ_θ to the normal emittance ϵ_N can be determined to be

$$\frac{\epsilon_\theta}{\epsilon_N} = \frac{[\rho_{2\nu}(\theta'\theta) - 1][1 - \rho_{2\nu}^N \rho_{1\nu}^N \exp^{-2\,t_o}][\rho_{1\nu}(\mu) \exp^{-2\,t_o/\mu} - 1]}{[1 - \rho_{2\nu}(\theta'\theta)\rho_{1\nu}(\mu) \exp^{-2\,t_o/\mu}][\rho_{2\nu}^N - 1][\rho_{1\nu}^N \exp^{-2\,t_o} - 1]}$$

The expression was derived for the case where the geometrical depth is much greater than one wavelength, and so does not consider interference effects. Since interference waves were not observed for the coatings in this work, it is assumed that the above expression is a good approximation for the systems studied under this program.

Section 3
MATERIAL DESCRIPTION

3.1 VACUUM DEPOSITION SOURCE MATERIAL

The materials used for deposition were high purity silver and alumina as described in Ref. 1.

3.2 SUBSTRATES

The substrates used were:

- Sapphire (Insaco Inc., Quakerstown, Pa.)
  1 in. diameter – 1/32 in. thick, pitch-polished 80-50
  Finished both sides
- Polyester (Dupont Mylar D) Film
  0.0075 in. thick
- Fused Silica
  Pitch-polished 80-50
  Finished both sides

It was expected that a substrate cut from an ingot will be generally the same as another substrate cut from the same ingot by the same manufacturer, within the general published specifications for that grade of material. However, there can be variations in optical properties across the cross-section and along ingot axis.

It has been reported (Ref. 4) that there are considerable variations of room temperature transmissivity in specimens of fused silica. The variations are with manufacturer, optical grade, ingot number,and within an ingot. This was not investigated as test results showed that these variations were not significant in the solar spectral region.

The substrates were cut and polished by a commercial optical finisher (Esco Products, Oak Ridge, N. J.), from Commercial Ingots of fused silica. The sizes, material sources,and grades are shown in the following:

Supplier	Grade	Size (in.)	Thickness (in.)
Corning	7940 Industrial	1 in. diam.	.008
		1 in. square	.008
		1 in. diam.	1/32
		1/2 × 1	0.008
	7940 uv	1/2 × 1	0.008
General Electric	151	1/2 × 1	1/32
Amersil	T20 Suprasil II	1/2 × 1	1/32
Thermal American	Spectrosil B	1/2 × 1	1/32

The Calorimetric Emittance Apparatus was used to determine the total hemispherical emittance of the dielectric coatings in the temperature range from 300°K to 800°K. This apparatus used a blackbody receiver, which was kept at a much lower temperature than the radiating sample (sample temperature was approximately three times greater than blackbody temperature) to intercept the sample's radiant energy.

The apparatus shown in Fig. 4-1 consists of an upper supporting structure for the sample and blackbody receiver and a vacuum-tight stainless steel shell which surrounds the supporting structure. Vacuum access to the shell is provided through a one-inch stainless steel tube welded in place. The entire apparatus is fitted to a 30-liter double walled Dewar. The Dewar's inner section can be filled with either liquid nitrogen or liquid hydrogen, thus providing a low temperature thermal ground for the apparatus. With liquid nitrogen in the Dewar's guard section the shell assembly can be kept completely covered with a cryogenic fluid for a period of 24 hours.

The 1 in. square sample mounting block is clamped to the supporting structure through a 1/4-in. O.D. with a 10 mil wall thickness stainless steel tube which is silver soldered to its back face. Sample temperature is controlled from 300°K to 800°K by an 80 watt Wattohm cartridge heater press-fitted into the sample heating block. Surrounding the sample heating block is a cooled radiation shield. This shield prevents radiation from the sides of the heating block from reaching the 2-1/2 in. diam. blockbody. The surface of the shield is covered with an aluminum foil tape to further minimize radiation exchange between the shield and blackbody receiver.

The blackbody receiver consists of a 2-1/2 OD by 1-1/4 in. high aluminum shell assembly, open at one end. Its interior is fitted with an array of 1-1/4 in. long aluminum tubes and painted with "Cat-a-Lac" flat black paint. The geometry of the assembly coupled with the high absorptance of the black paint produces a very effective blackbody with an absorptance > 0.98 for the thermal radiation involved in this experiment. The blackbody is clamped to the supporting structure through a 1/4 in. rod or tube of varying materials. By using different thermal links, the

Section 4

EQUIPMENT AND APPARATUS

4.1 DEPOSITION EQUIPMENT

The equipment used for this work is the electron beam evaporation system as previously reported (Ref. 1).

A modification was made to the system that permitted the insertion and withdrawal of a resistance-heated silver evaporation crucible during the deposition process.

The crucible was mounted to a linear vacuum seal rod that protruded into the existing, but modified, shutter-shield system of the present configuration. An adapter ring was inserted between the existing metal vacuum chamber and the pyrex viewing cylinder. This modification was essential to the deposition of silver films with no contamination from the crucible structure.

4.2 TEST EQUIPMENT

4.2.1 Proton Radiation Apparatus

Test equipment that was used for proton radiation was existing (Ref. 5) Minor modification of the proton radiation equipment was necessary for tests to be conducted at 700 °K.

4.2.2 Hemispherical Emittance Apparatus

Modification was made to the hemispherical emittance apparatus for the measurements up to 800 °K. This apparatus was previously described (Ref. 1); but as there have been numerous other modifications since the previous reporting, a discussion of these is presented.

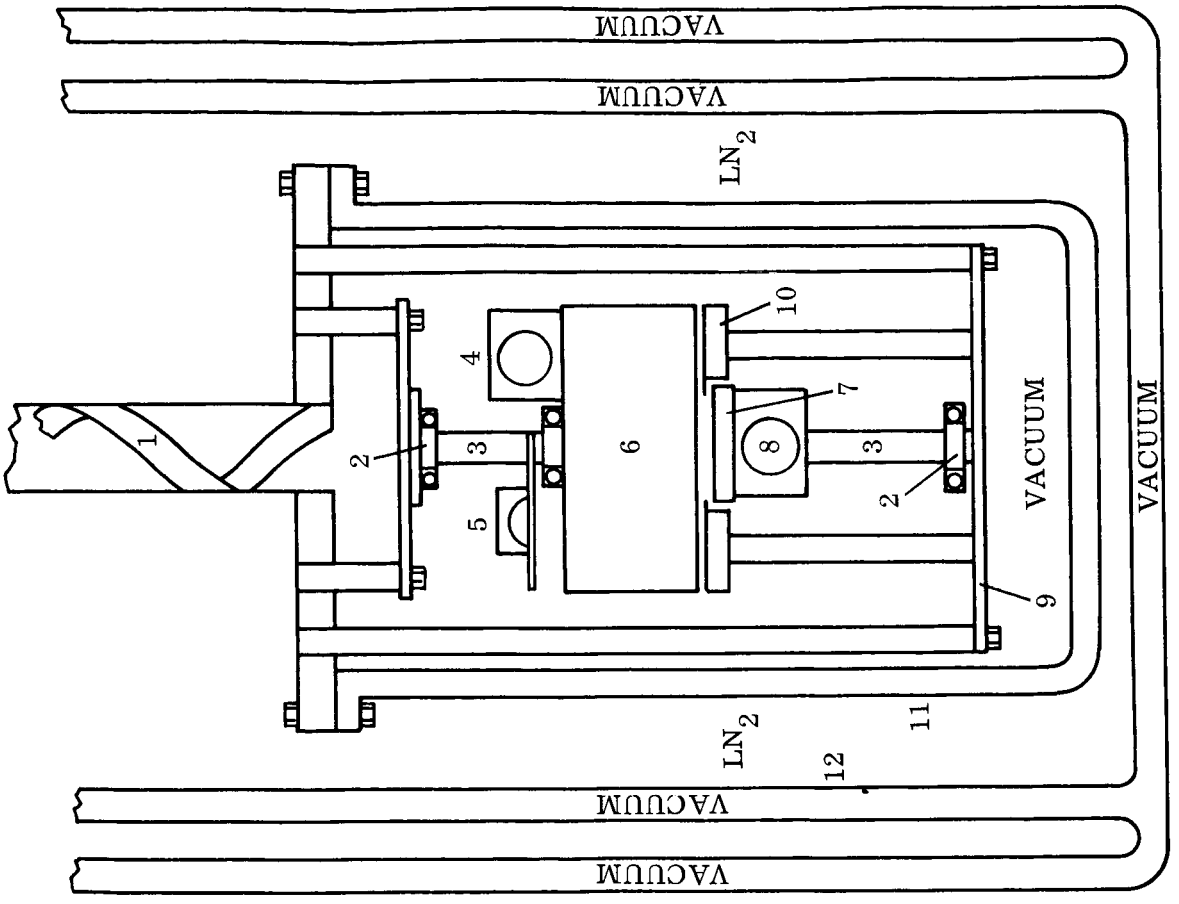

1 COPPER RADIATION STRAP
2 CLAMP
3 THERMAL LINK
4 RESISTANCE HEATER
5 PLATINUM RESISTANCE THERMOMETER
6 BLACKBODY RECEIVER
7 COPPER SAMPLE MOUNT
8 SAMPLE HEATER
9 COPPER SUPPORTING STRUCTURE
10 SAMPLE MASK
11 VACUUM TIGHT CYLINDER
12 DOUBLE WALL DEWAR

Fig. 4-1 Cryogenic Emittance Apparatus

blackbody equilibrium temperature can be controlled. The blackbody back face is equipped with a Rosemont Engineering Company 104 AH1 platinum resistance thermometer. Using calibration data suppled by Rosemont, this thermometer is accurate to ±0.1°K. For calibration purposes the blackbody is also equipped with a 200 ohm carbon resistor heater.

The experimental procedure consisted of performing calibration measurements and emittance measurements.

Emittance Measurements. The 1 in. square fused silica and stainless steel sample substrates were clamped into place on the copper heating block using six 15 mil diameter steel spring wire clips. Radiation from the lips was effectively reduced by the sample mask that overlapped the sample just enough to cover the lips. Sample temperature readout was provided by a chromel-alumel thermocouple cemented to the sample's front face using a ceramic adhesive. Because of the small diameter of the wire used for the thermocouple (3 mil), and the size of the adhesive bead the thermocouples effect on the emittance of the high emittance OSR was neglected. However, for the low emittance silver – Al_2O_3 coatings, the thermocouple was cemented to the substrate prior to vacuum deposition.

The blackbody and sample assemblies were clamped into place with approximately 30 mils separating their front faces. The shell assembly was then bolted together and lowered into the 30-liter Dewar. While at room temperature the apparatus was evacuated to a pressure of $< 10^{-5}$ Torr. Liquid nitrogen was added to the space surrounding the shell assembly and to the Dewar's guard section. A pressure $< 10^{-6}$ Torr was realized.

The sample heater was set for the desired sample temperature. The thermal energy leaving the sample's front face was intercepted by the blackbody and raised its temperature. For the series of measurements the blackbody thermal link was chosen so that the blackbody's temperature was always < 1/3 sample temperature.

This minimized the radiation energy lost by the blackbody both to the blackened shell walls and to the sample front face. Once sample and blackbody temperature equilibrium were attained (< 18 hours) their respective temperatures were recorded. Sample thermocouple voltages were measured using a Leeds and Northrup K-3 potentiometer. The four lead technique was used for blackbody temperature measurements. Current measurements were made using a precision standard resistor in conjunction with the K-3 potentiometer.

Calibration Measurements. In order to define the thermal energy reaching the blackbody from the sample it was necessary to calibrate the blackbody receiver. This was done by allowing the sample to cool to cryogenic bath temperature and supplying heat energy to the receiver through a 200-ohm carbon resistor heater mounted to its black face. Once blackbody thermal equilibrium was attained, the power dissipated in the carbon resistor was measured and the temperature (thermometer resistance) was recorded. The process was then repeated for different power levels and a curve of blackbody temperature vs. power input to the blackbody was generated. This technique produced a very reproducible curve, since not only the blackbody thermal link but all the leads to the resistance mounted on its back face were thermally grounded to the cryogenic bath. Power measurements were made using the four-lead technique with the K-3 potentiometer and a precision standard resistor.

Emittance Calculation. The emittance calculations were made in the following manner. From the emittance measurements procedure, it follows that with a sample radiating, the heat-flux that reached the blackbody thermal link was equal to the radiated sample energy that was absorbed by the blackbody minus the radiated blackbody energy that was either absorbed by the sample or the chamber walls.

Therefore:

$$Q_L = A_S \sigma T_S^4 F_{SB} \frac{\epsilon_s a_b}{\epsilon_s + a_b - \epsilon_s a_b} - A_B \sigma T_B^4 F_{BS} \frac{\epsilon_b a'_s}{\epsilon_b + a'_s - \epsilon_b a'_s} - Y_S \qquad (4.1)$$

And, during calibration the heat flux reaching the link was:

$$Q_L = Q_c - Q_R \tag{4.2}$$

where

$$Q_R = A_B \sigma T_B^4 F_{BS} \frac{\epsilon_b a''_s}{\epsilon_b + a''_s - \epsilon_b a''_s} + Y_c$$

Thus, Q_L has been defined with a radiating sample present, and with a calibration heat input Q_C ; so, for corresponding blackbody temperatures we have by combining Eqs. (4.1) and (4.2)

$$A_S \sigma T_S^4 F_{SB} \frac{\epsilon_s a_b}{\epsilon_s + a_b - \epsilon_s a_b} - A_B \sigma T_B^4 F_{BS} \frac{\epsilon_b a'_s}{\epsilon_b + a'_s - \epsilon_b a'_s} - Y_S$$

$$= Q_c - A_B T_B^4 F_{BS} \frac{\epsilon_b a''_s}{\epsilon_b + a''_s - \epsilon_b a''_s} - Y_c \tag{4.3}$$

At corresponding blackbody temperatures $Y_S = Y_C$, thus, these terms are cancelled.

The second terms on either side of the Eq. (4.3) effectively cancel each other, even though $a''_j \neq a's_j$ since $T_B << T_S$. This assumption introduces an error estimated at less than 0.5%.

Finally,

$$Q_c = A_S \sigma T_S^4 F_{SB} \frac{\epsilon_s a_b}{\epsilon_s + a_b - \epsilon_s a_b} \tag{4.4}$$

The emittance E_j can now be calculated, since all the terms in Eq. (4.4) are known including a_b, which was calculated using an iterative process and data obtained by substituting a blackbody radiator identical to the blackbody receiver for the sample. The emittance, or absorptance, of the blackbody from 80°K to 260°K, was found to be 0.98 ± 0.01.

Error Analysis. Most of the errors in this measurement technique can be attributed to errors in measuring the terms in Eq. (4.4)

$$\text{Probable Error} = \sqrt{\left(\frac{\Delta Q_c}{Q_c}\right)^2 + \left(\frac{4\Delta T_s}{T_s}\right)^2 + (F_{SB})^2 + \left(\frac{\Delta d_b}{a_b}\right)^2}$$

where

Low Emittance Measurements Figs. 6-1, 6-2	High Emittance Measurements Fig. 6-3
$\frac{\Delta Q_c}{Q_c} \approx 1.0 \times 10^{-2}$ or 1%	$\frac{\Delta Q_c}{Q_c} \approx 1.0 \times 10^{-2}$ or 1.0%
$\frac{\Delta T_s}{T_s} \approx 1.5 \times 10^{-2}$ or 1.5%	$\frac{\Delta T_s}{T_s} \approx 1.5 \times 10^{-2}$ or 1.5%
$F_{SB} \approx 4.0 \times 10^{-2}$ or 4.0%	$F_{SB} < 1.0 \times 10^{-3}$ or negligible
$\frac{\Delta a_b}{a_b} \approx 1.0 \times 10^{-2}$ or 1.0%	$\frac{\Delta a_b}{a_b} \approx 1.0 \times 10^{-2}$ or 1.0%

The estimated error for the low emittance values presented in this report in 300°K to 800°K temperature range is 6%. The estimated error for the high emittance values is 4%. The trend of the emittance curves and the relative position of the curves with respect to each other are at a higher confidence level, because of consistency in thermometer placement and measurement technique.

4.3 SPECTRAL REFLECTANCE/EMITTANCE APPARATUS

The measurements at wavelengths less than 1.8 μ are spectral normal reflectance measurements obtained with a Cary Model 14 Spectrophotometer and Integrating Sphere Reflectometer attachment. The data at wavelengths longer than 1.8 μ are near normal (θ = 20°) spectral reflectance measurements obtained with a Gier-Dunkle Model HC-300 Heated Cavity Reflectometer in conjunction with a Perkin-Elmer Model 98 Monochrometer and a Brower Model 129 Chopper-Amplifier system. The latter measurements were made point-by-point at integral wavelengths from 2 to 25 μ, and were repeatable to within ± 0.002. The absolute accuracy of each measurement is believed to be on the order of ● 0.005 except for the measurements at λ = 2μ. At this wavelength an error due to a temperature difference between the cavity walls ($T_w \approx 1030°K$) and the platinum reference fin can cause the reflectance measurements to be high by as much as 0.020 (see Ref. 6); however, in comparison with the Cary data and with data for freshly evaporated silver reported by Hass (Ref. 7) the possible error does not appear to be greater than 0.010. At wavelengths longer than 4 μ, the error from this source drops to less than 0.010. The entrance-port error (Ref. 6) for these samples at θ = 20° is negligible because of their highly specular reflectance characteristics.

4.4 OPTICAL MEASUREMENT EQUIPMENT

All necessary equipment for optical measurements was available. A multiple beam interferometer (Sloan Instruments, M100) was used for measuring the thin film thickness. As some of the films were the order of hundreds of angstroms, optical flats were co-deposited with the specimen substrates in order to facilitate measurements of the absolute deposition thickness with sufficient accuracy.

Section 5
EXPERIMENTAL PROCEDURES

5.1 OPTICAL FILM DEPOSITION

The fabrication of the OSR's (Optical Solar Reflectors) and first surface silver films was accomplished by conventional vacuum evaporation techniques using resistance heated tungsten evaporation boats for silver and Inconel. Electron beam heating was used for evaporating alumina Great care was taken to minimize silver deposition contamination by shielding the crucible.

5.2 SUBSTRATE PREPARATION

The procedure for cleaning the substrates was common to all depositions. The substrates were cleaned in an ultrasonic cleaner. Substrates were immersed in a Freon emulsion (DuPont TWD-602) for two minutes. This solvent removes both organic and inorganic soils. This was followed by two separate rinses in Freon TF. A final rise in boiling Freon TF was done. This leaves the substrate clean and free of any "water-spots" or dust particles. Substrates were immediately placed in the substrate holder after final rinse and the vacuum system was evacuated to deposition conditions.

5.3 DEPOSITION PROCEDURE

This procedure followed as before (Ref. 1). In the case of the deposition of silver films only in the range of 200 Å to 1000 Å and thin dielectric overlays, an optical flat was co-deposited in order to measure film thicknesses with accuracy.

5.4 ENVIRONMENTAL TESTING OF OPTICAL SURFACES

5.4.1 Ultraviolet Radiation

Specimens were radiated in a uv vacuum chamber (Ref. 1) for 500 ESH (equivalent sun-hours) at 700°K using a 1 kW A-H6 (PEK Laboratory Type C) mercury-argon high pressure lamp.

5.4.2 Proton Radiation

Proton radiation was accomplished in a system similar to the one described in Ref. 3. The Lockheed combined environmental chamber was used to simulate the environment of interest, which in this particular series of experiments was a proton-only environment. The equipment is so designed as to allow simulation of three separate environments, namely particle only, ultraviolet only, and particle-plus-ultraviolet. Dependent upon the sample holder used, ten to sixteen samples can be accommodated during one exposure.

The basic vacuum system is fabricated from 301 stainless steel which has been chemically polished on the internal faces. A stainless steel cryogenic shroud is within the main chamber so that the test sample table is almost completely enclosed when in the exposure position. Vacuum seals are either O ring (Viton) or metal (copper and indium). A water cooled oil diffusion pump is used to maintain vacuum. An optically dense, liquid nitrogen cooled, circular chevron trap separates the diffusion pump and the exposure chamber. Rough pumping on the diffusion pump is carried out with a mechanical pump which is separated from the diffusion pump by a molecular sieve trap. High vacuum pressures are measured by a nude trifilament ionization gauge.

The sample holders, which have facilities for low or high temperature bombardments (i.e., 77 °K to 750 °K) are fabricated from high purity oxygen free copper. In this particular series of experiments where no in situ measurements were made, the sample table was placed in position in the main chamber prior to pump down. After completion of the bombardment the main chamber was allowed up to atmosphere and the table removed. In the case of exposures requiring in situ measurements the table is admitted to the main chamber through a vacuum lock attached to the main chamber.

The particle source which is mated to the chamber consists of a radio frequency ion gun which generates low energy protons (0 to 5 keV). The ion gun is supplied by Oak Ridge Technical Enterprise Corp. (ORTEC) and operates with an 80 mc oscillator, palladium leak, and focussing magnet. The beam is composed of H_1^+, H_2^+ and negligible H_3^+ ions. Approximately 85% of the beam was H_1^+ ions for the reported tests. The proton source used during the test had a flux of 2×10^{12} p/cm^2-sec. A movable 1 cm^2 copper button, was used as a detector of particle intensity at the sample location.

5.5 OPTICAL MEASUREMENTS

5.5.1 Reflectance

Spectral reflectance was measured from 0.275 to 1.8μ on the Cary Spectrophotometer. Solar absorptance was calculated from the integration of the Cary trace, which is adjusted for variations in solar flux at various wavelengths.

5.5.2 Directional Spectral Reflectance

Directional spectral reflectance properties were measured over the spectral range of 2 to 25μ with a Gier Dunkle Heated Cavity Absolute Reflectometer. The measurements were performed with samples prepared on 1 in. diameter discs.

Section 6
EXPERIMENTAL RESULTS AND ANALYSIS

6.1 THIN FILM DEPOSITION PARAMETERS

6.1.1 Silver Adhesion

Evaporative depositions of silver on glass and fused silica substrates were made in order to establish the controlling deposition parameters to obtain maximum solar reflectance. The adhesion of silver to the substrate was first investigated to determine the critical factors in achieving adhesion in accordance with an arbitrary scotch tape test.

This test consisted of pulling a piece of 1/2 in. wide scotch tape (minimum of 1/4 square inch contact area on silver film) perpendicular to film surface with a 6 to 8 oz force. No film separation from substrate area was considered acceptable adhesion.

The results of the adhesion tests were that adhesion was poor regardless of the substrate preparation or evaporation rate if the substrates were not heated in vacuum. It appears that unless water is desorbed from the substrate surface poor adhesion results.

The 1000 Å of Inconel overlayed on the silver to protect the silver from corrosion has no apparent effect on the silver adhesion. However, for thicker films of Inconel the stress in the Inconel film may adversely affect the silver adhesion. There were not a sufficient number of samples to verify this. Ultrasonic cleaning of the substrates with Freon TF had no advantage in adhesion over a water detergent cleaning.

Heating the substrate to 350°K for 10 minutes by argon discharge resulted in much improved adhesion but with a 40% failure rate out of 8 specimens. This was true whether the silver was deposited with the substrate at 350°K or cooled to 320°K before evaporating.

Tests were run for adhesion with substrates heated to 405°K and then cooled to 322°K before depositing the silver. Adhesion was good under these conditions (6 samples per run using fused silica substrates). The best adhesion was achieved by heating substrates to 495°K. The substrates were then cooled to approximately 325°K before evaporation of the silver began. Chamber pressure was 2 to 5×10^{-7} Torr during evaporation. These tests were repeated using deposition rates 2 Å/sec, 20 Å/sec, 100 Å/sec, and 200 Å/sec. Adhesion was good with one failure at 20 Å/sec and 100 Å/sec. At 2 Å/sec there was a failure of three out of six. With the exception of the very slow deposition rate of 2 Å/sec, there appears to be no rate dependency on adhesion. There is essentially no differente in α (0.049) when the silver was deposited on a substrate at elevated temperature 400°K as compared to a substrate that is cooled and then deposited. It is expected that this would not be true at higher substrate temperatures (in excess of 600°K).

It was noted that even though the silver did not peel from the substrate with scotch tape, some silver (and Inconel) could be removed from the surface as a result of the tape test. This is not noticable unless the substrate is brightly backlighted. This metal removal occurs on samples prepared by Optical Coating Labs (OCLI)* and NASA-Ames as well. This is due to the poor adhesion of silver to itself. It is expected that this could be minimized by depositing a thicker coating of Inconel (the order of a micron) so that the superior mechanical properties of Inconel would become effective.

The adhesion of silver to fused silica in order to obtain minimum absorption resulted in marginal silver adhesion even under optimum conditions. In addition, there was occasionally a disconcerting lifting of the silver from the silica substrates when the OSR was immersed in water. This was inconsistent even in OSR's deposited under identical conditions. (This also happens with commercial OSR's).

The marginal silver adhesion was considered unsatisfactory and was investigated further. The substrates were treated in three ways prior to silver deposition. These were by undercoating with a thin film of evaporated (1) silica, (2) magnesium fluoride, and (3) hydrofluoric acid etching of the fused silica. The fused silica

*Santa Rosa, California

overcoated with silicon dioxide of various thicknesses (300 Å, 800 Å, and 1000 Å) showed much poorer adhesion than silver deposited directly on the fused silica substrate. The overcoatings with magnesium fluoride (300 Å and 800 Å) resulted in poor silver adhesion with the 300 Å Mg F coating and marginal adhesion with the 800 Å coating.

The third treatment was etching the side to be coated with approximately 40% (by weight) room temperature hydrofluoric acid for, (1) 1 min, and (2) 2 min. The silver adhesion was excellent in both etching cases. Silver could not be removed by scotch tape by any manner of rough treatment. Immersion in water had no effect.

The visual appearance with the 1 minute etch was very minor etch lines. The 2 minute etch resulted in an etched and pitted surface, comparable to a very light "frost" appearance. The 1 minute etched OSR and the co-deposited non-etched OSR had the same (identical Cary traces) α_s values of 0.046.

The 2 minute etch resulted in an increase of absorptance of the order of 1% in the infrared (0.6 to 1.8 range). A very light etch appears to be adequate for excellent adhesion.

The etched substrates were heated to 400°K and then cooled to 340°K prior to silver deposition.

It is likely that good adhesion could be obtained by heating substrate to the order of 800°K and cooling to 400°K prior to silver deposition without the necessity of HF etching. Inasmuch as the particular substrate holder used had no heater; substrate heating was done by argon ion bombardment. Substrate temperatures in excess of 500°K were not practical for this system.

6.1.2 Deposition Rate

The α_s of the OSR's was independent of the rate of deposition in the range of 2 Å/sec to 200 Å/sec. There were some very minor differences in the Cary traces in the UV region (0.28 to 0.38 μ).

6.1.3 Substrate Material

There were no significant differences in α_s of the OSR's using differing grades of fused silica.

6.2 SILVER FILM STABILITY

The stability of silver films overcoated with thin alumina films in the range of 200 Å to 1000 Å was evaluated. A thorough corrosion evaluation was outside of the scope of this program. A highly accelerated corrosion test was performed. This test was probably one of the most rigorous for silver films.

The test consisted of suspending samples in a closed container. The samples were immersed in a hydrogen sulfide vapor of high humidity (close to 100% relative humidity). This was accomplished by using a solution of ammonium polysulfide $(NH_4)_2 S_x$ in water. This was such a corrosive atmosphere that it caused a bare silver film to blacken in a fraction of a second. The results of the test are shown in Table 6-1.

Table 6-1

CORROSION OF ALUMINA OVERCOATED SILVER*

Alumina Thickness (Å)	α_s (Before Exposure)	α_s (After 1 hr Exposure)
–	0.047	0.677 (film failure)
210	0.055	0.064
550	0.054	0.060
955	0.054	0.059

*1200 Å silver on fused silica substrates.

6.3 ULTRAVIOLET ENVIRONMENTAL TEST RESULTS

The ultraviolet radiation tests of 500 equivalent sun-hr exposure at 700°K were performed on OSR's using various grades of fused silica substrates. As some degradation occurred fused silica specimens, uncoated and coated, were subjected to 700°K for the same period as the ultraviolet test in order to determine if the effect were due to ultraviolet, elevated temperature, or silver diffusion and/or silver recrystallization.

The results of the ultraviolet test (Table 6-2) showed that there is a small increase in α_s for the OSR using various grades of fused silica after ultraviolet radiation of 500 ESH at 700°K. The differences between grades of fused silica is insignificant. The transmittance decrease of the order of 1% in the fused silica (Table 6-3) is attributed to ultraviolet at 700°K as there was no change in transmittance at 700°K without ultraviolet exposure. Comparing results with a commercial OSR (on the basis of one sample only), the initial α_s (0.049) of the commercial OSR was higher. However, it did not change with ultraviolet exposure. The prepared test samples did change from 0.044 to 0.054 on the average. It is postulated that the commercial OSR's may have a dielectric layer deposited before applying the silver coating. This may decrease the rate of silver diffusion into the fused silica at elevated temperatures.

6.4 PROTON RADIATION TEST RESULTS

Prepared OSR specimens of various grades of fused silica were subjected to proton radiation. The specimens were exposed to 2 keV protons of 1×10^{16} ρ/cm^2, 1×10^{17} ρ/cm^2, and 5×10^{17} ρ/cm^2 with substrate temperatures of 400°K, 530°K, and 700°K. None of the samples showed any optical damage under these test conditions. Commercial OSR (OCLI) specimens were also radiated and similarly showed no change.

One specimen group (700°K substrate temperature) received some surface contamination during exposure from 1×10^{16} ρ/cm^2 to 1×10^{17} ρ/cm^2. This was shown to be contamination due to a sample removal procedure.

Table 6-2

SOLAR ABSORPTANCE OF OSR (OPTICAL SOLAR REFLECTOR)

Material Fused Silica (2nd Surface Silver Reflector)	UV Test (500 ESH: 50 hr at 10-Sun Intensity at 700°K)		Elevated Temperature Test (no UV) (48 hr at 700°K)	
	Pre-UV	Post-UV	Pre-UV	Post-UV
1. Corning 7940 UV grade 0.008 in. thick	0.044	0.055		
2. Corning 7940 Industrial Grade 0.008 in. thick	0.044	0.054	0.044	0.048
3. Corning 7940 Industrial Grade 1/32 in. thick	0.043	0.053		
4. General Electric 1/32 in. thick	0.044	0.060		
5. Suprasil II (Amersil) 1/32 in. thick	0.045	0.053		
6. Spectrasil B (Thermal American) 1/32 in. thick	0.046	0.053		
7. OSR Commercial (Optical Coating Labs, Inc.)	0.049	0.049	0.049	0.049

Table 6-3

SOLAR TRANSMITTANCE OF FUSED SILICA (UNCOATED)

Material (Fused Silica)	UV Test (500 ESH: 50 hr at 10-Sun Intensity at 700°K:)		Elevated Temperature Test (no UV) (48 hr at 700°K)	
	Pre-UV	Post UV	Pre-700°K Exposure	Post Exposure
1. Corning 7940 UV Grade 0.008 in. thick	0.934	0.925		
2. Corning 7940 Industrial Grade 0.008 in. thick	0.938	0.928	0.938	0.938
3. Corning 7940 Industrial 1/32 in. thick	0.938	0.932		
4. General Electric 151 1/32 in. thick	0.941	0.929		
5. Suprasil II (Amersil) 1/32 in. thick	0.937	0.932		
6. Spectrasil B (Thermal American) 1/32 in. thick	0.936	0.931		

6.4.1 Measurement Results

The total hemispherical emittance of the thin dielectric films in the temperature range from 300°K to 800°K is presented graphically in Figs. 6-1, 6-2, and 6-3. Figure 6-4 shows the hemispherical emittance of the alumina overcoated silver surfaces on fused silica substrates as a function of Al_2O_3 thickness.

6.4.2 Analysis of Results

The OSR showed a significant decrease in emittance with increasing temperature. The data presented herein agreed closely with calculated values of the normal emittance in the temperature range from 300°K to 500°K. The total hemispherical emittance of the alumina overcoated silver coatings did not appear to be a function of substrate material. However, it was a strong function of alumina overcoating thickness, as shown in Figs. 6-1, 6-2, and 6-3.

In accumulating the hemispherical emittance data, it was discovered that in the higher temperature ranges (600°K to 800°K) reliable data could be generated only if temperature readout was taken from some point on the surface of the radiating sample. In addition, great care had to be exercised to assure even sample clamping pressure. The problem was most acute in the case of the highly emitting OSR surfaces. Here, a trial run was made with the OSR attached using a polyimide film with a silicone adhesive on both sides. Temperature readout was provided at a point in the heating block 1/16 in. below the radiating surface. Using this temperature, the "effective" emittance was calculated and found to be about 5% lower than the actual emittance due to the ΔT between the temperature readout point and the OSR's radiating face. The disparity between the "effective" emittance and actual emittance was thus a function of the conductance between the temperature readout point and the sample's radiating face. This disparity was much larger than 5% when mechanical clamping was used to hold the OSR in place.

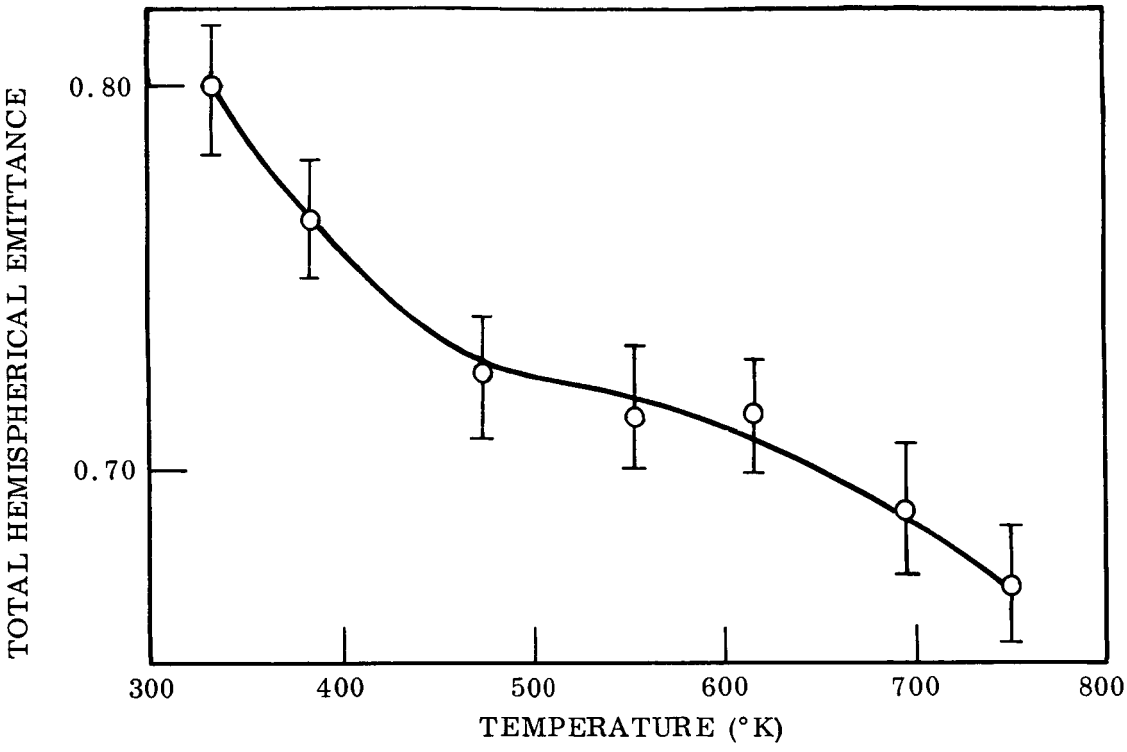

Fig. 6-3 Hemispherical Emittance as a Function of Temperature Silver Backed OSR

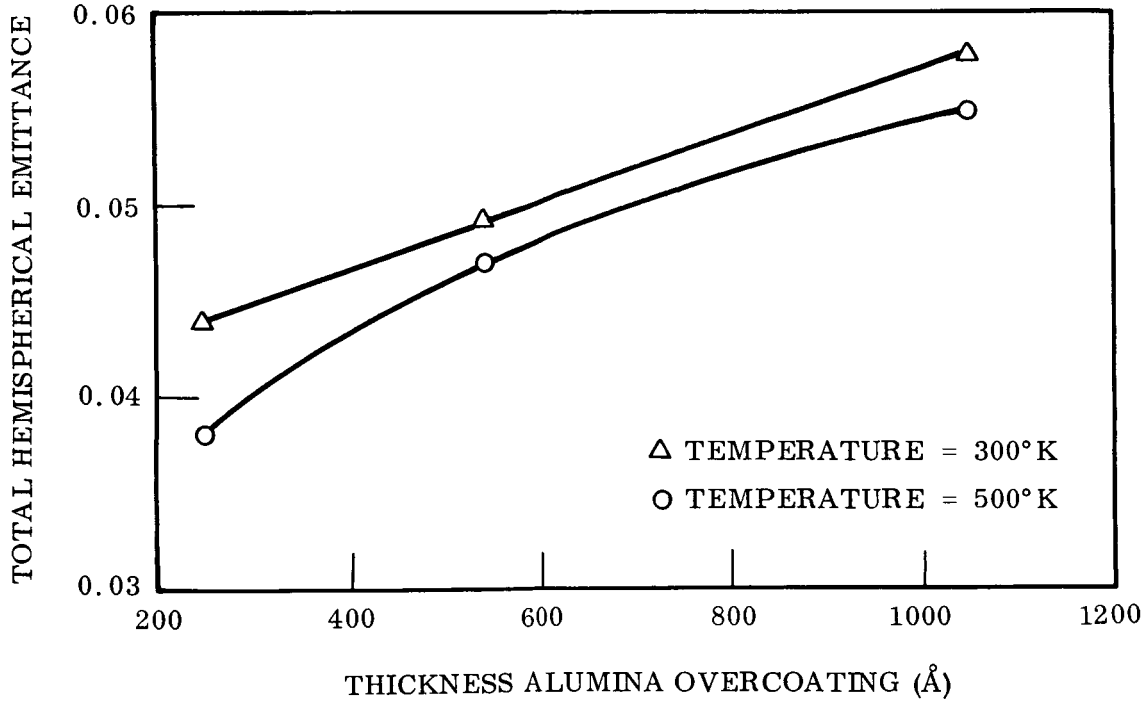

Fig. 6-4 Hemispherical Emittance as a Function of Alumina Overcoating Thickness – Fused Silica Substrates

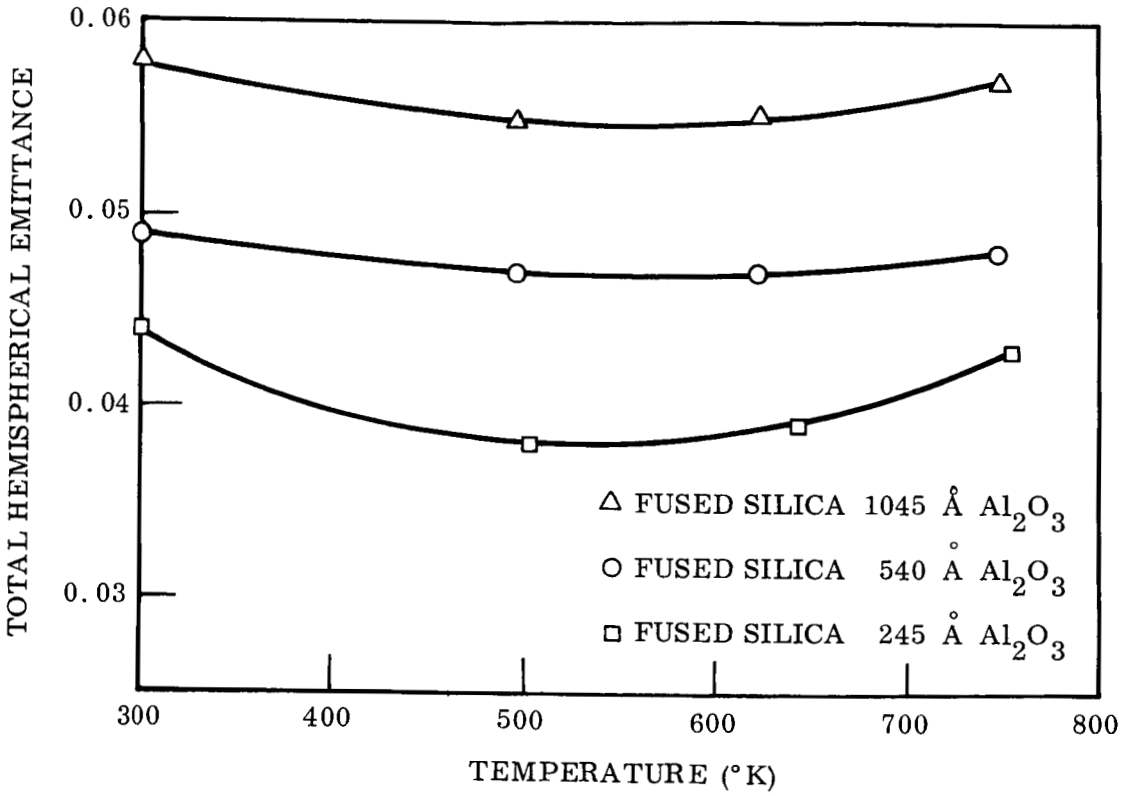

Fig. 6-1 Hemispherical Emittance as a Function of Temperature Alumina Overcoated Silver on Fused Silica Substrates

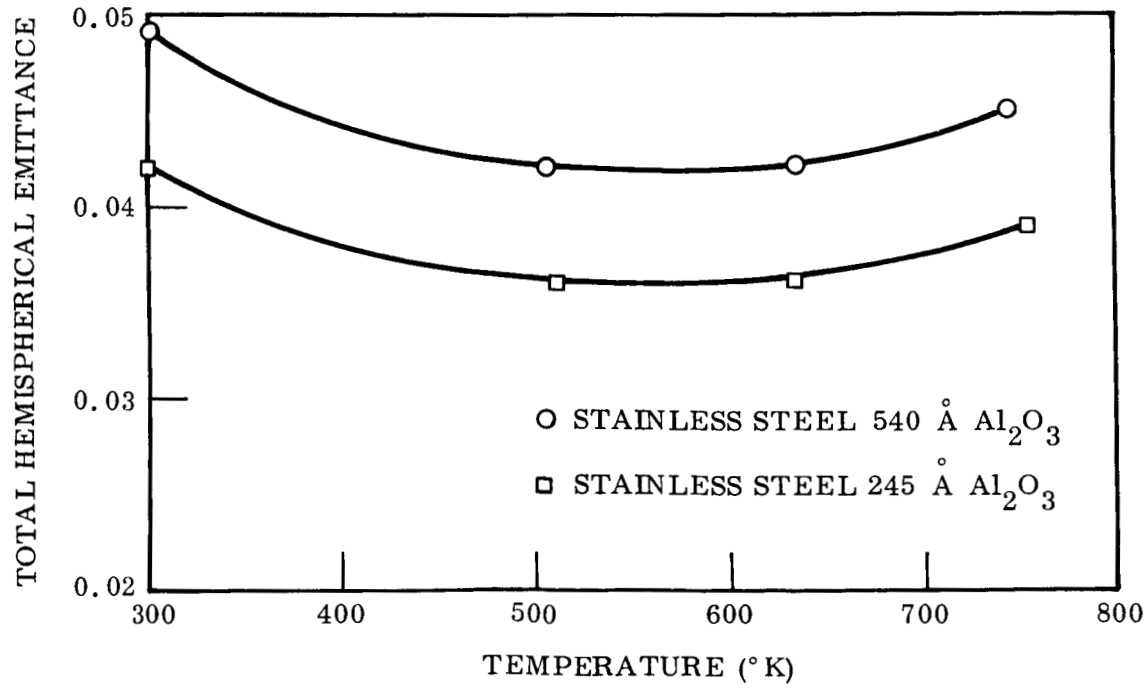

Fig. 6-2 Hemispherical Emittance as a Function of Temperature Alumina Overcoated Silver on Stainless Steel Substrates

These results suggest that if the OSR and other thermal control surfaces using fused silica substrates are to be used in the temperature range beyond the capabilities of the elastomeric adhesive, then, extreme care must be exercised in mechanically mounting the panels so that they will behave as designed. In essence, the ΔT between the OSR and the surface to which it is attached must be kept to a minimum, or at least to a consistently measurable quantity. In the case of the OSR this is a monumental task since extreme or uneven pressure will break the delicate panels.

6.5 SPECTRAL REFLECTANCE/EMITTANCE MEASUREMENTS

The room temperature spectral reflectance for three different alumina-coated silver-on-quartz samples is shown in Fig. 6-5. The data shown at wavelengths less than 1.8 μ are spectral normal reflectance measurements (Figs. 6-6, 6-7, and 6-8).

The results in Fig. 6-5 indicate that increasing the thickness of the alumina overcoat from 0 to 1000 Å has only a slight, if any, effect on the normal, infrared reflectance of silver. The differences in reflectance values for the 210 Å and 550 Å samples are generally less than the range of uncertainty for the measurements and is therefore not significant. Reflectance values for the 955 Å sample are generally from 1/4 to 1/2 percent lower than the others except in the 5 to 7 μ region, where they are the same, and in the 10 to 12 μ region where the presence of an absorption band is apparent. These results are consistent with the results reported by Hass (Ref. 8) for the overcoatings of alumina and SiO on Al where no significant increase in total normal emittance was observed until the thickness exceeded 1000 Å.

Variations in the spectral directional reflectance of the alumina coated specimens at room temperature are shown in Figs. 6-9, 6-10, 6-11, and 6-12 at wavelengths of 5, 11, 15, and 20 μ. These figures show the relative spectral directional reflectance, $\rho(\theta, \lambda)/\rho(\theta_N, \lambda)$, for each of the specimens at each of the wavelengths. The measurements were made with the Gier-Dunkle reflectometer by recording the detector signal as the sample viewing angle was changed from near normal to 80°

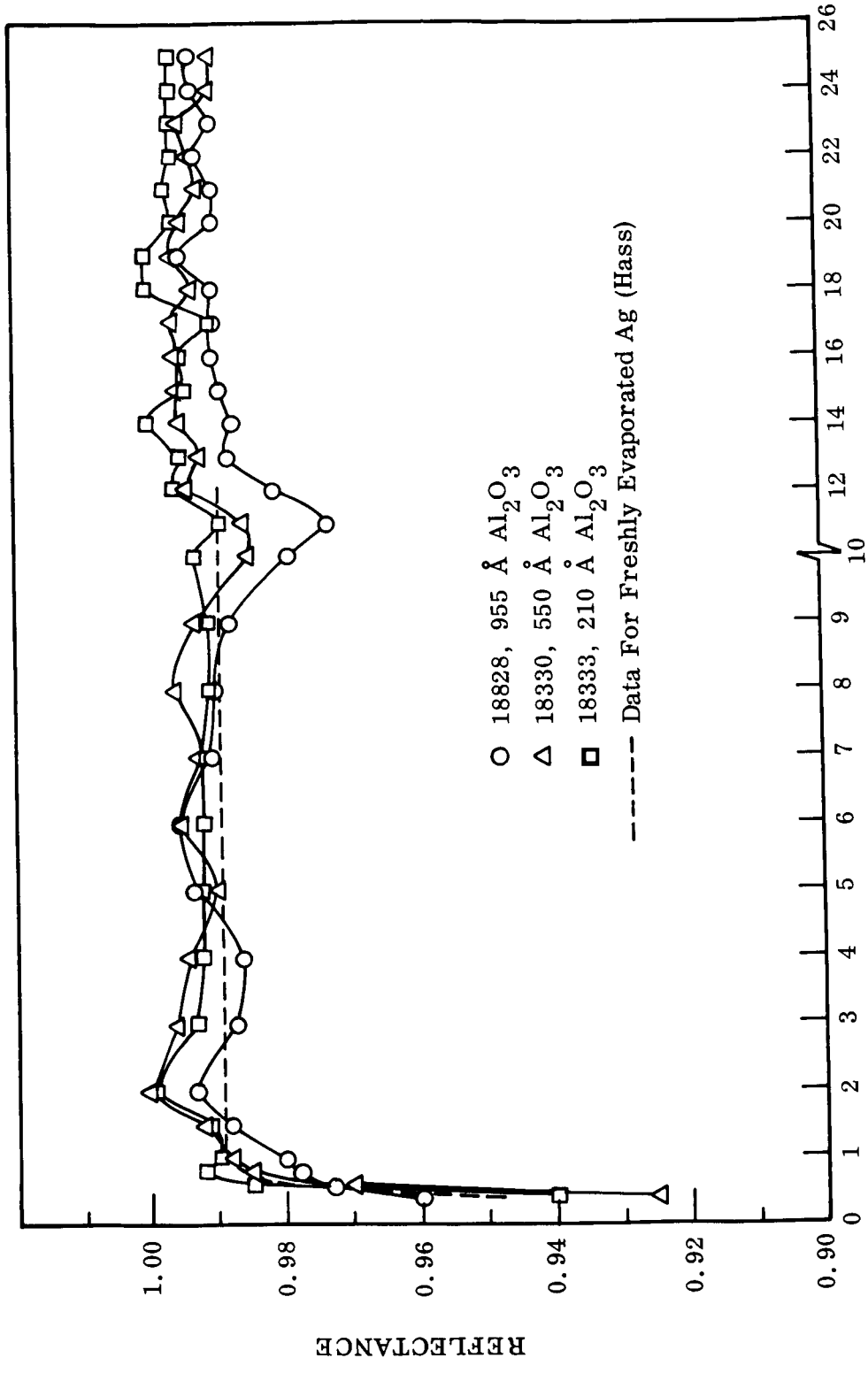

Fig. 6-5 Reflectance as a Function of Wavelength, Aluminum Oxide Films on Silver (Fused Silica Substrate)

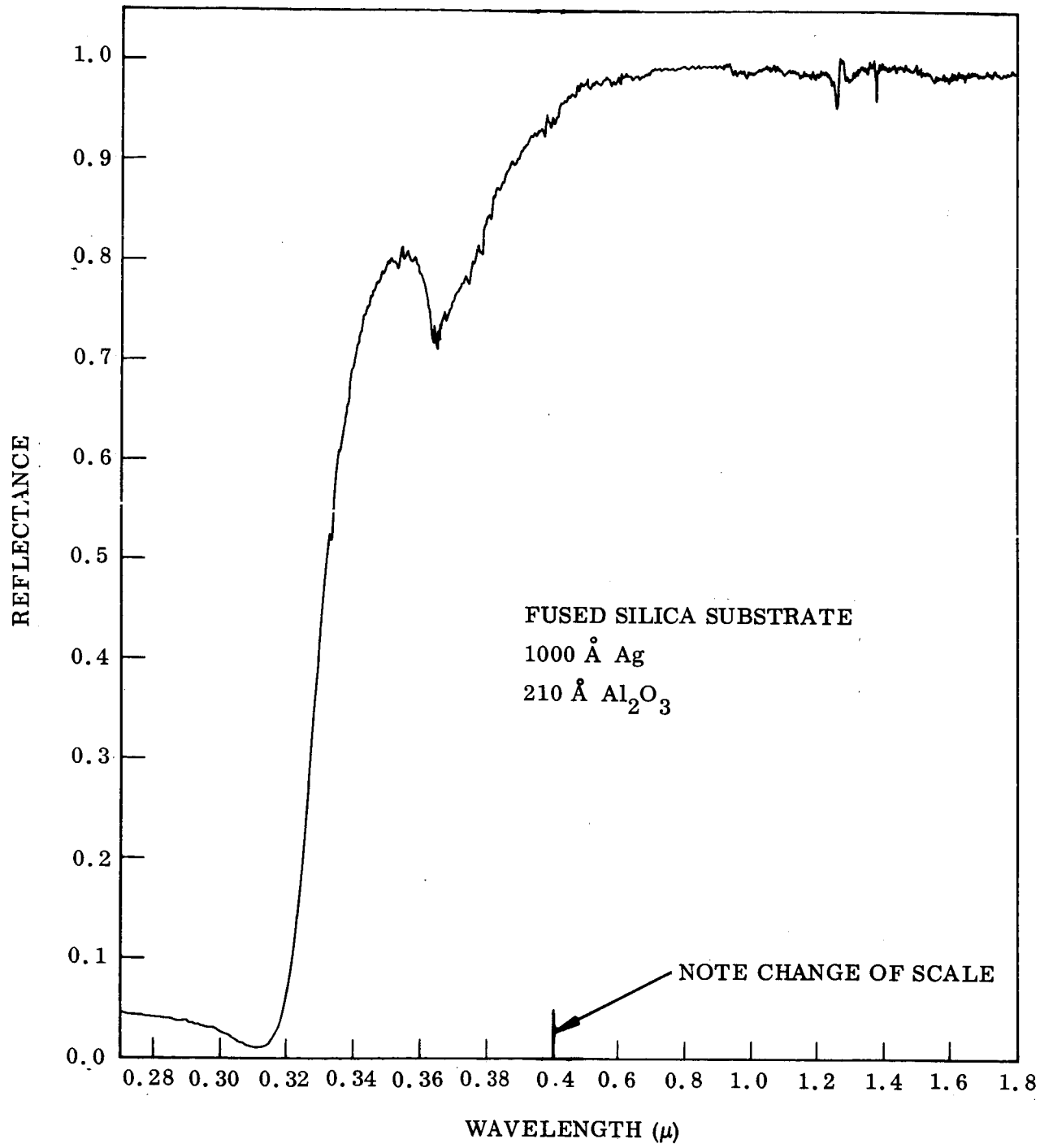

Fig. 6-6 Spectral Reflectance of 210 Å Aluminum Oxide Film on Silver at Less Than 1.8 μ

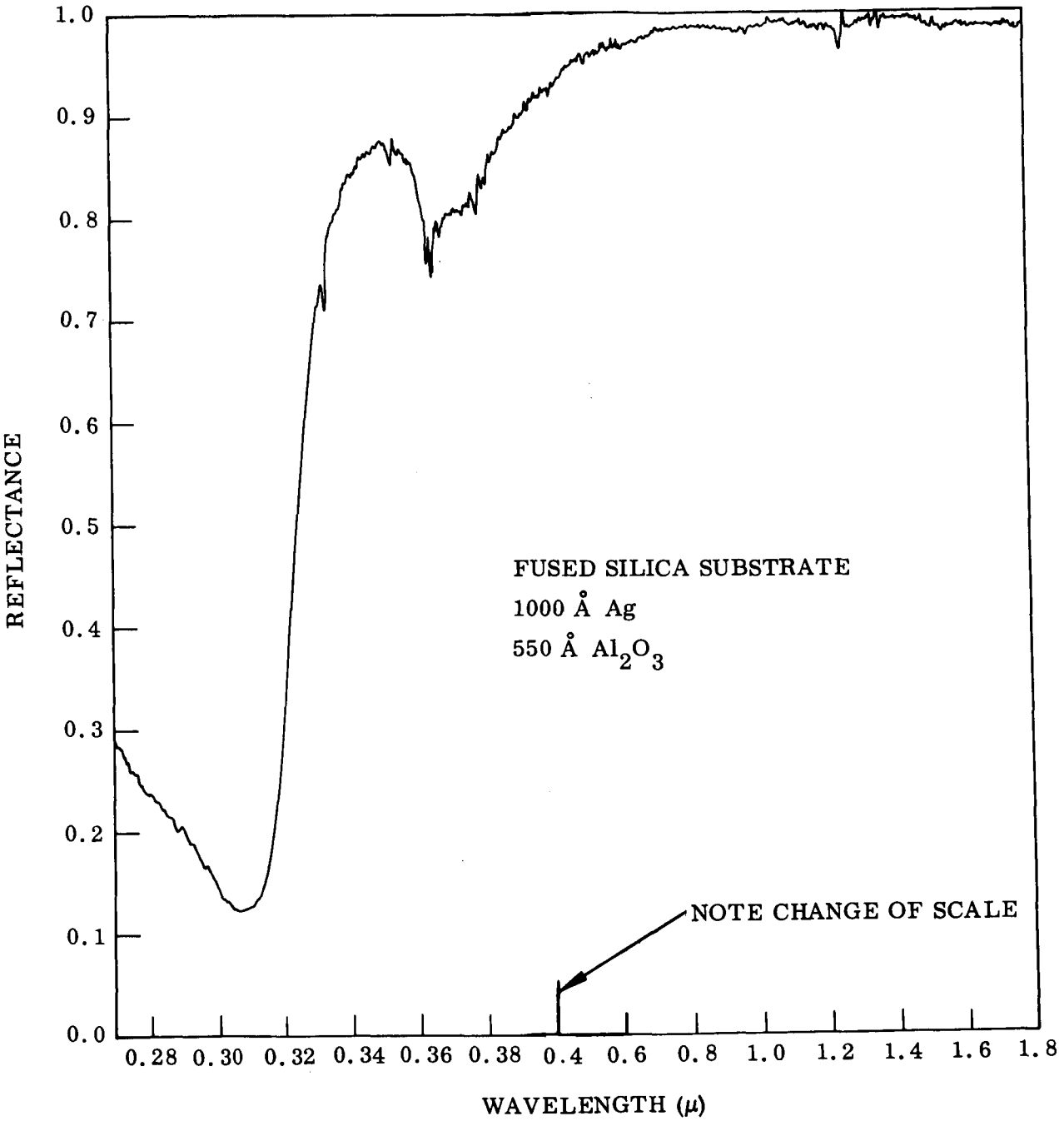

Fig. 6-7 Spectral Reflectance of 550 Å Aluminum Oxide Film on Silver at Less Than 1.8 μ

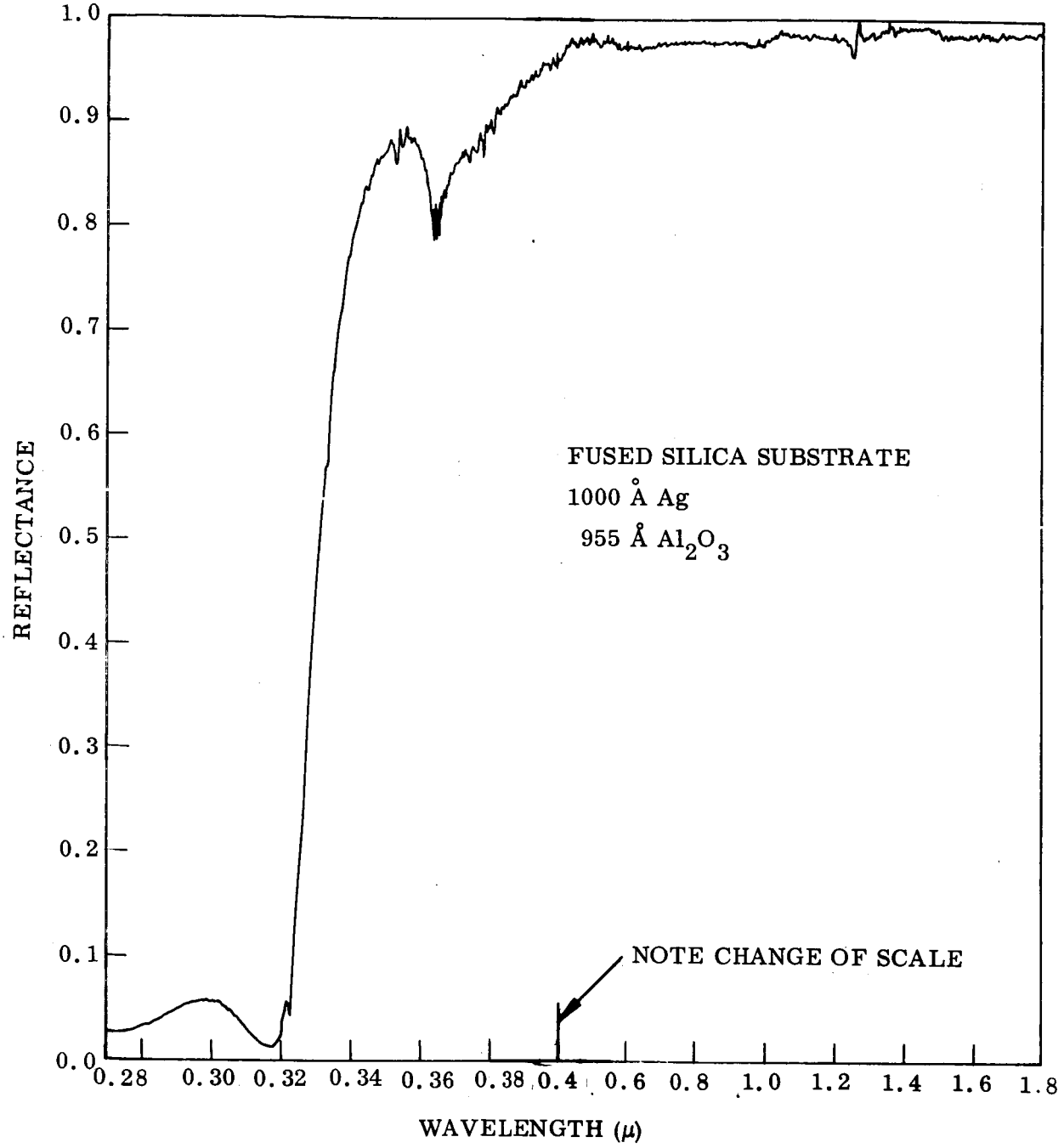

Fig. 6-8 Spectral Reflectance of 955 Å Aluminum Oxide Film on Silver at Less Than 1.8 μ

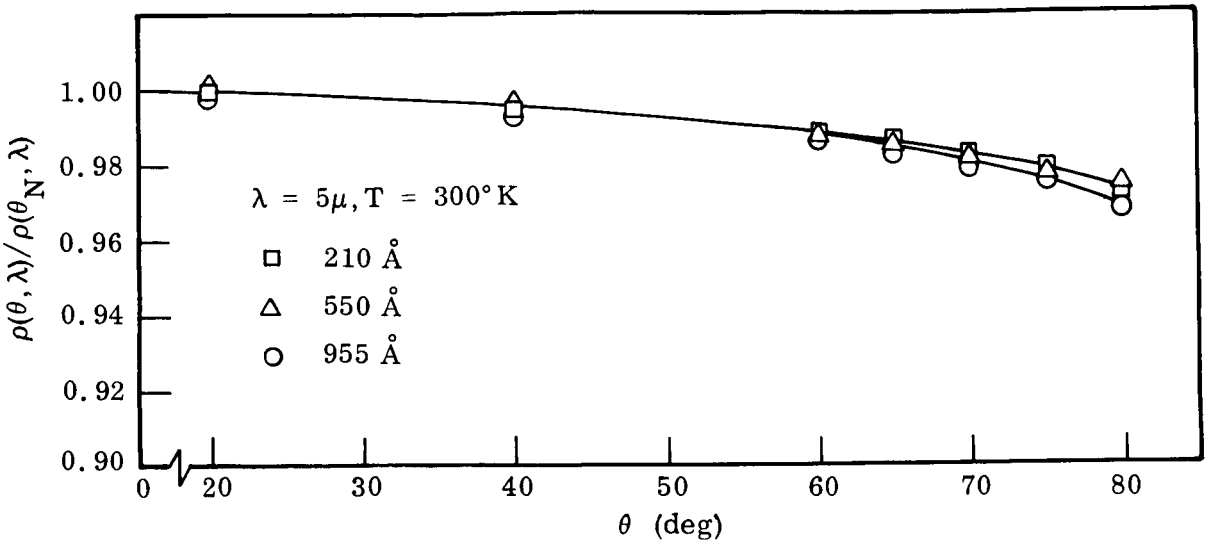

Fig. 6-9 Relative Directional Reflectance of Ag/Al_2O_3 Samples at 5 μ

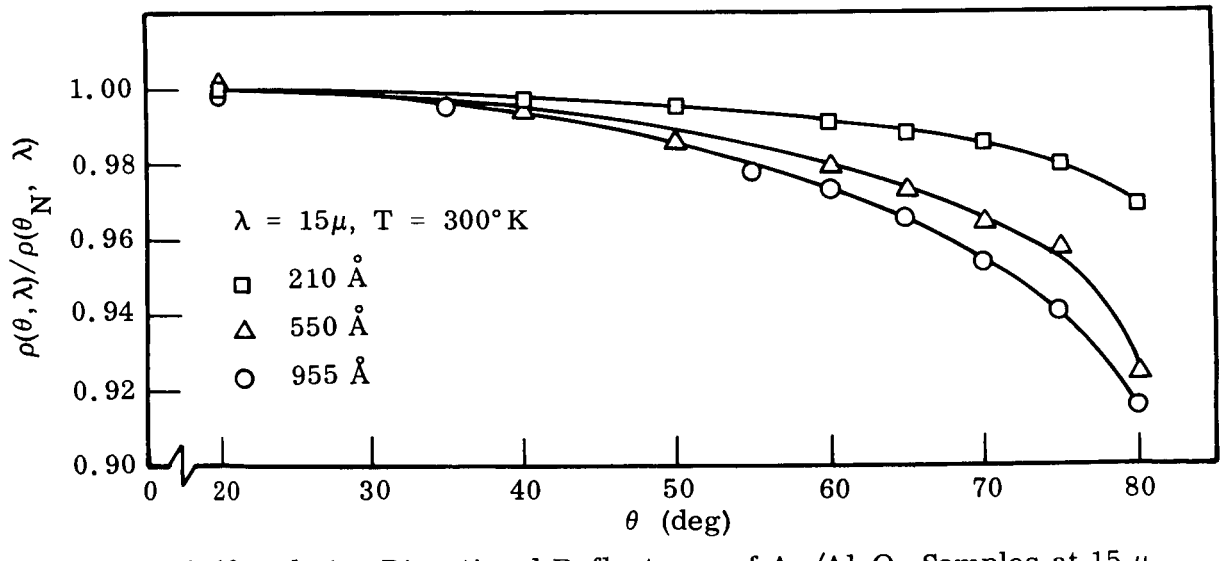

Fig. 6-10 Relative Directional Reflectance of Ag/Al_2O_3 Samples at 15 μ

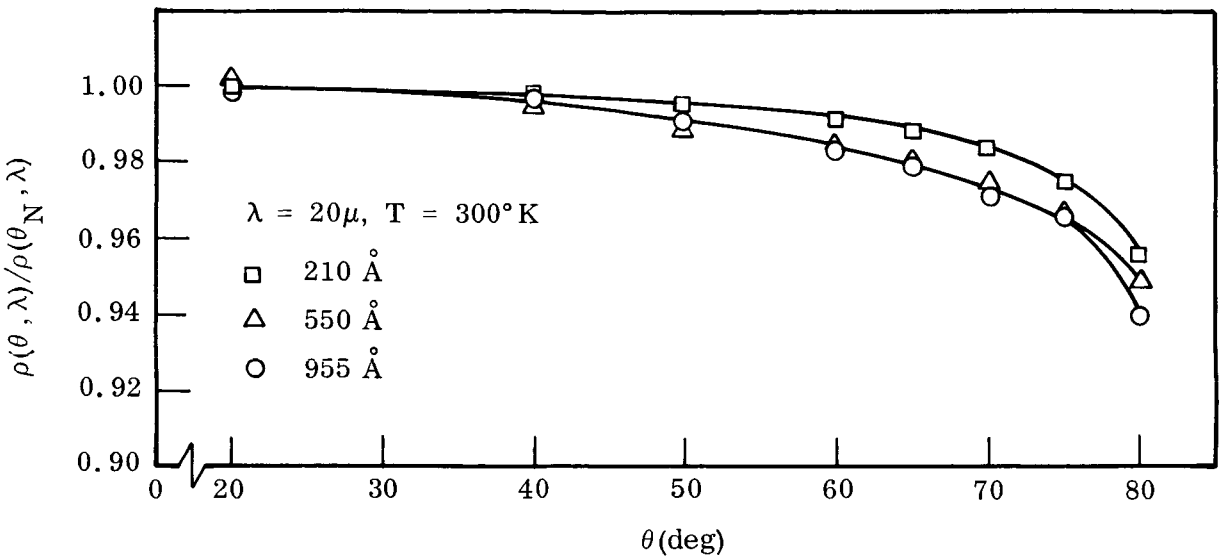

Fig. 6-11 Relative Directional Reflectance of Ag/Al_2O_3 Samples at 20 μ

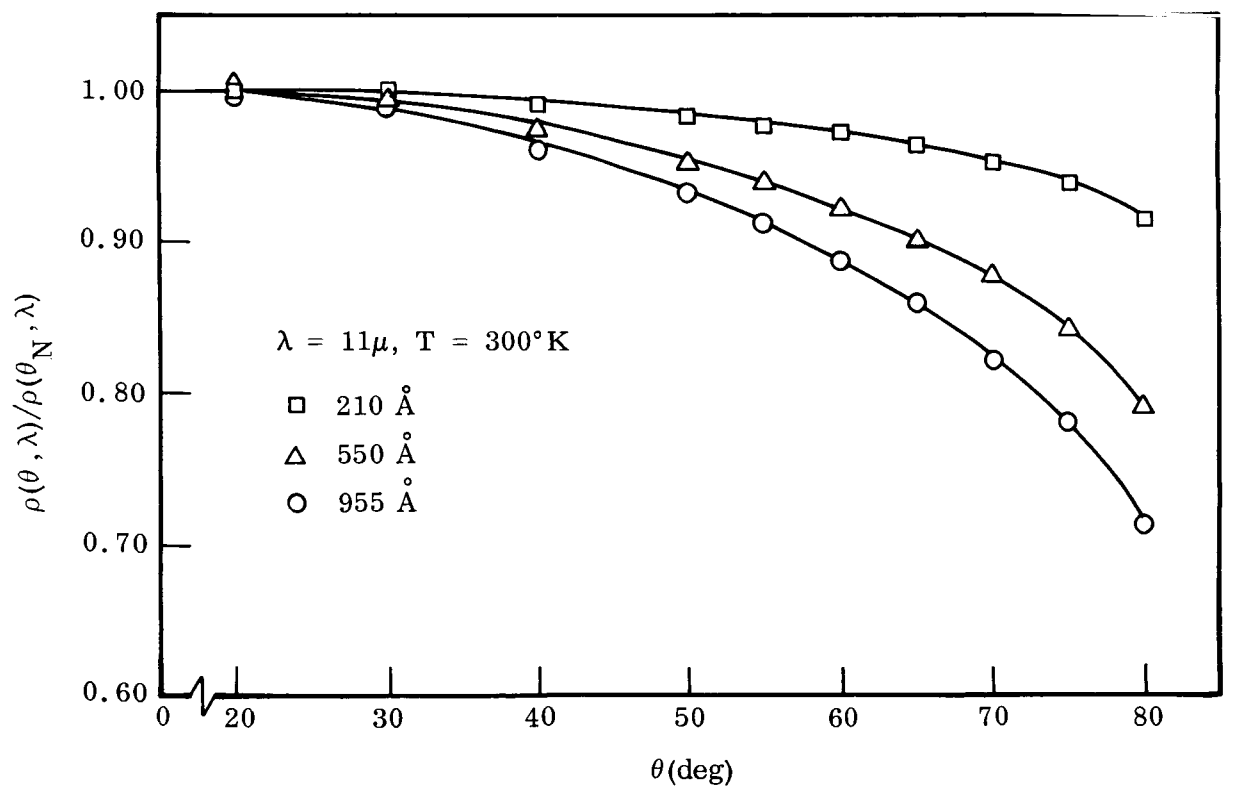

Fig. 6-12 Relative Directional Reflectance of Ag/Al_2O_3 Samples at 11 μ

off normal. These signals, $V(\theta)$, were then normalized to the signal value of $\theta = 20°$ to obtain the relative directional reflectance values, assuming that $V(\theta, \lambda)/V(\theta = 20°, \lambda) = \rho(\theta, \lambda)/\rho(\theta_N, \lambda)$. Directional data for θ values greater than 80° were not possible because edges of the sample holder began to be viewed.

The directional reflectance results show that significant changes occur as the thickness the alumina coating increases from 210 to 955 Å. The change is wavelength dependent and is most sensitive at $\lambda = 11\ \mu$ where the directional reflectance of the 955 Å coating at 80° falls off to 71% of the normal reflectance value as compared to a drop to 92% for the 210 Å coating. Less sensitivity is observed at $\lambda = 15\ \mu$ and $\lambda = 20\ \mu$ where the 80° reflectance values are all above 90% of the normal reflectance values. At $\lambda = 5\ \mu$ the difference between samples is so slight that it is of questionable significance.

The insensitivity of the directional reflectance with coating thickness at $\lambda = 5\ \mu$ may seem surprising because the optical thickness factors, $\frac{nt}{\lambda}$, are more than twice those at $\lambda = 11\ \mu$ and 4 times those at $\lambda = 20\ \mu$. The results are understood, however, when the following factors are considered:

- n and k for the silver substrate are significantly less at 5 μ than at 11 μ (approximately 12.5 and 75 respectively at 11 μ as compared with 2.5 and 35 at 5 μ). Consequently, the relative directional reflectance curve for uncoated silver is considerably flatter at $\lambda = 5\ \mu$ than at 11μ, and hence less sensitive to change.
- The relative index for the Ag/Al_2O_3 interface is much closer to 1 at $\lambda = 5\ \mu$ than at $\lambda = 11\mu$ (e.g., $n(Ag)/n(Al_2O_3)$ increases with λ since $n(Al_2O_3)$ does not change significantly between 5 and 11 μ).
- The absorptance of Al_2O_3 at $\lambda = 5\ \mu$ is small in comparison with its absorptance of $\lambda = 11\mu$ (Ref. 4).

A summary of the reflectance and emittance results derived from the near-normal and relative directional reflectance determinations for each sample is presented in Table 6-4. In column 3 of the table, values for the spectral normal reflectance of the samples are listed under the designation ρ_N. These are the measured values of near-normal spectral reflectance as shown in Fig. 6-5 and, as stated previously, are believed accurate to within ± 0.005. In column 5 of the table, values for the spectral normal emittance of the samples are listed under the designation ϵ_N. These values are obtained from the ρ_N values in column 3, assuming $\epsilon_N = 1 - \rho_N$; consequently, the uncertainty is still ± 0.005. Because of the low spectral emittance characteristics of these samples, the 0.005 uncertainty inherent in the measurements results in a relative uncertainty in ϵ_N of from 20% to 100%.

Table 6-4

SPECTRAL REFLECTANCE AND EMITTANCE CHARACTERISTICS OF Al_2O_3-COATED SILVER SAMPLE(e)

Wavelength (μ)	Thickness Al_2O_3 (Å)	ρ_N(a)	ρ_H/ρ_N(b)	ϵ_N(c)	ϵ_H(d)	ϵ_H/ϵ_N
5	210	0.992	0.993	0.008	0.015	1.9
	550	0.990	0.993	0.010	0.017	1.7
	955	0.993	0.992	0.007	0.015	2.1
11	210	0.989	0.983	0.011	0.028	2.5
	550	0.986	0.953	0.014	0.060	4.3
	955	0.973	0.931	0.027	0.094	3.5
15	210	0.994	0.994	0.006	0.012	2.0
	550	0.994	0.987	0.006	0.019	3.2
	955	0.990	0.983	0.010	0.027	2.7
20	210	0.996	0.994	0.004	0.010	2.5
	550	0.995	0.990	0.005	0.015	3.0
	955	0.990	0.990	0.010	0.020	2.0

(a) ρ_N values are the near-normal ($\theta = 20°$) measured values shown in Fig. 1.

(b) ρ_H/ρ_N values are those obtained by numerical integration of the relative spectral directional reflectance curves shown in Figs. 6-6 through 6-9.

(c) $\epsilon_N = 1 - \rho_N$.

(d) $\epsilon_H = 1 - \rho_N(\rho_H/\rho_N)$.

(e) Fused silica substrate

In column 4 of the table, values for the hemispherical-to-normal spectral reflectance ratios are listed under the designation ρ_H/ρ_N. These values are obtained by numerical integration of the relative directional reflectance curves shown in Figs. 6-9 through 6-11, where:

$$\rho_H/\rho_N = 2\int_1^0 f(\theta)\cos\theta\, d(\cos\theta) \qquad (6.5)$$

[Note: For a perfect lambertian (cosine) reflector, $f(\theta) = 1$ for all values of θ and $\rho_H/\rho_N = 1$ from Eq. (6.5).]

The ρ_H/ρ_N values listed in Table 6-4 were determined from 21 readings from the $\rho(\theta,\lambda)/\rho\theta_N,\lambda)$ curves at angles corresponding to 0.05 increment changes in $\cos\theta$ from $\cos\theta = 1$ to $\cos\theta = 0$. For θ values greater than 80° (four required), extrapolated values for $f(\theta)$ were required; however, the error involved is small because of the low values for $\cos\theta (0 \leq \theta \leq 0.20)$. Consequently, the overall uncertainty in ρ_H/ρ_N is small and is believed to be on the order of ± 0.002.

In column 4 of the Table 6-4, values for the spectral hemispherical emittance of the samples are listed under the heading ϵ_H. These values are obtained from the ρ_N and ρ_H/ρ_N values, assuming that:

$$\epsilon_H = 1 - \rho_N(\rho_H/\rho_N) \qquad (6.6)$$

and the maximum uncertainty in ϵ_H is on the order of ± 0.007. Most of the uncertainty can be attributed to the 0.005 uncertainty in the ρ_N determination.

Values for the hemispherical-to-normal spectral emittance ratio are listed in the last column of Table 6-4 under the heading ϵ_H/ϵ_N. These ratios vary from a minimum of 1.7 to a maximum of 4.3 whereas the theoretical ϵ_H/ϵ_N ratios for an uncoated silver surface would be between 1.3 and 1.4. For high reflectance specimens such

as these, the uncertainty in experimental determinations of ϵ_H/ϵ_N is high and is almost all attributable to the uncertainty in the ρ_N determination. For example (Table 6-5), if the ρ_H/ρ_N value for the 210 Å coated sample at $\lambda = 11\ \mu$ (0.983) is assumed to be correct, then an uncertainty of ± 0.005 in the ρ_N determination (0.989 ± 0.005) produces an uncertainty of ± 0.6 in the ϵ_H/ϵ_N ratio (i.e., 2.5 ± 0.6), and the uncertainty approaches infinity as ρ_N approaches 1 (i.e., as ϵ_N approaches 0).

Table 6-5

EFFECT OF A ± 0.005 UNCERTAINTY IN ρ_N ON THE ϵ_H/ϵ_N DETERMINATION FOR THE 210 Å COATED SAMPLE AT $\lambda = 11\ \mu$

ρ_N	ρ_H/ρ_N	$\epsilon_H = 1 - \rho_N(\rho_H/\rho_N)$	ϵ_H/ϵ_N
0.989 - 0.005 = 0.984	0.983	0.033	3.0
0.989	0.983	0.028	2.5
0.989 + 0.005 = 0.994	0.983	0.023	2.1

6.6 SPECTRAL TRANSMITTANCE OF SILVER FILMS

Spectral transmittance measurements were performed on silver films deposited on fused silica, sapphire and Mylar substrates. The Mylar thickness was 0.0075 inch whereas the other substrates were 0.031 inch thick. The deposition parameters are as follows:

Silver Film Thickness (Å)	Deposition Rate (Å/sec)
1080	52
900	75
710	51
620	69
490	81
290	72

Continuous traces of the transmittance of the various films were obtained over the wavelength range 0.28 to 1.8 μ, using a Cary Model 14 Spectrophotometer. On the silica and sapphire substrates, the silver films exhibited the typical transmittance window in the near ultraviolet region, with maximum transmittance at 3220 Å. The silver transmission spectrum on Mylar, however, was distorted due to the strong ultraviolet absorption of the substrate.

In Figs. 6-13, 6-14, and 6-15 are plotted the transmittances of the silver films on the three substrates as a function of thickness at 3200 Å, 3600 Å, and 4000 Å respectively. For equivalent silver thicknesses, the transmittance on Al_2O_3 consistently falls slightly below that of Ag on SiO_2. This effect is not unexpected since the front surface reflectance of Al_2O_3 is greater than that of SiO_2 due to the higher refractive index of the Al_2O_3. The Mylar data is consistent with those of the other substrates at 4000 Å but deviates at shorter wavelengths where substrate absorption becomes appreciable.

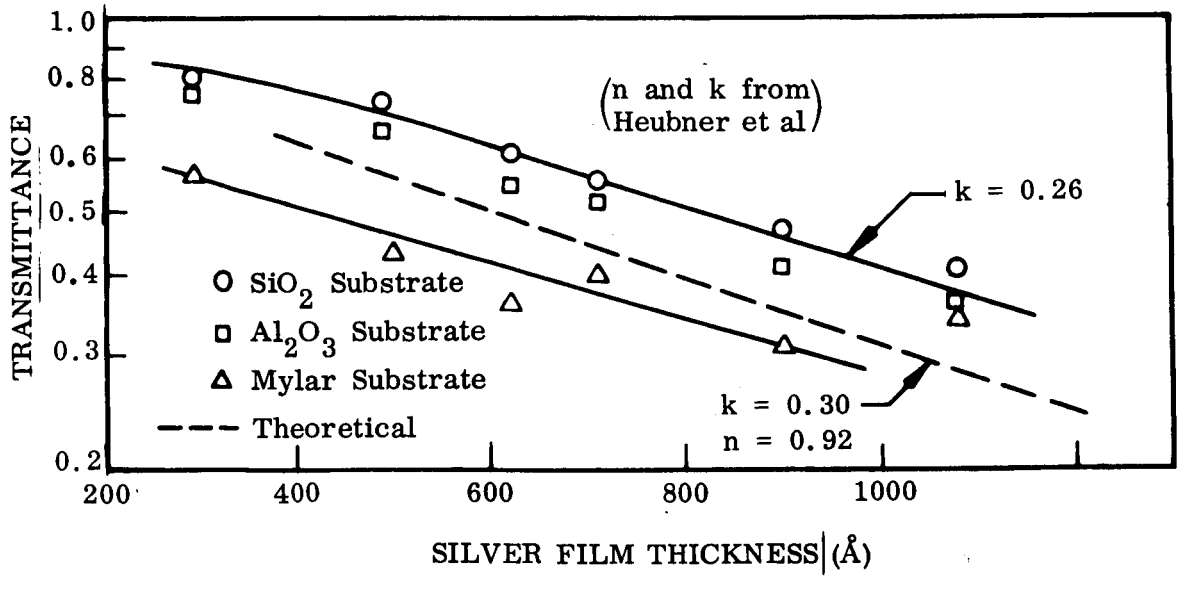

Fig. 6-13 Transmittance of Silver on Various Substrates as a Function of Film Thickness at λ = 3220 Å

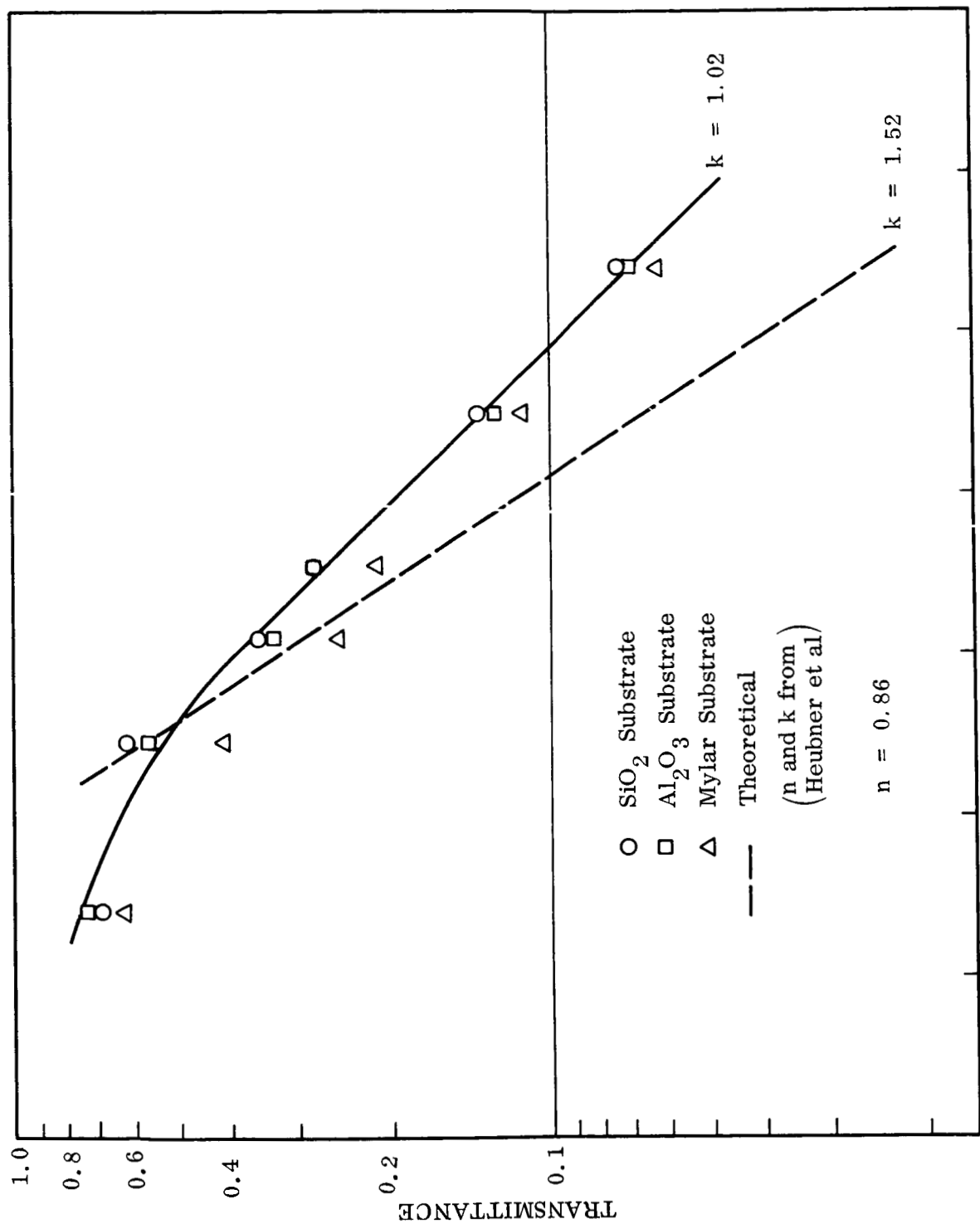

Fig. 6-14 Transmittance of Silver on Varicus Substrates as a Function of Film Thickness at λ = 3600 A

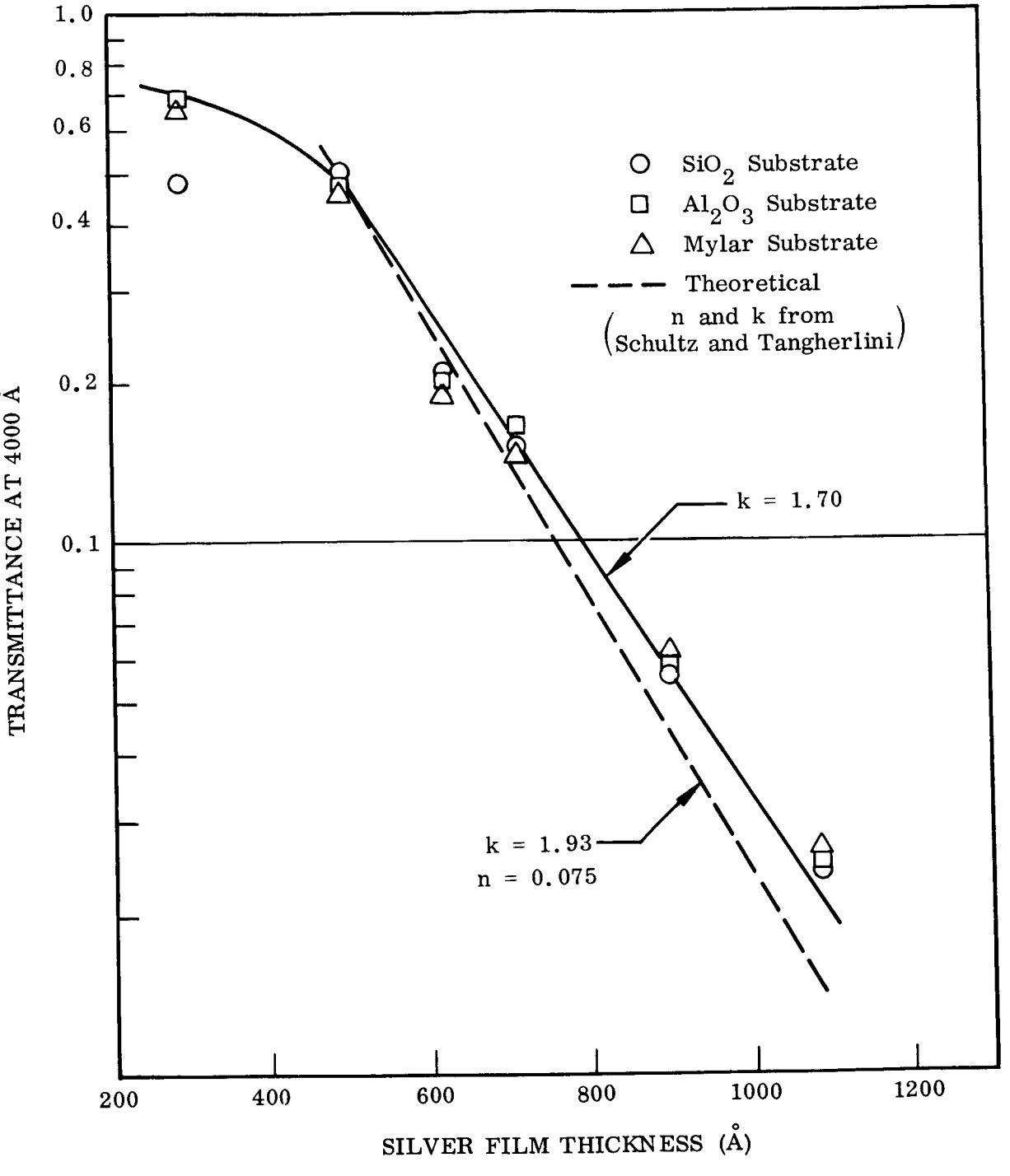

Fig. 6-15 Transmittance of Silver on Various Substrates as a Function of Film Thickness at λ = 4000 Å

As shown in Figs. 6-13, 6-14, and 6-15, the transmittance is an exponential function of the silver film thickness in the range 500 A to 1100 A at all wavelengths. Despite the fact that the absolute values of transmittance are substrate dependent, the slopes of the log T vs. thickness curves at a given wavelength are very nearly independent of the substrate.

From the variation of transmittance with thickness, it is possible to calculate values for the absorption index (k) of the silver films. For metal films of thickness greater than 300 to 400 A, in which the effects of multiple reflections are suppressed, the transmittance of a film of index n - ik is given by

$$T = \frac{16\, n_0 (n^2 + k^2) \exp(-4\pi kd/\lambda)}{[(n+1)^2 + k^2][(n_0 + n)^2 + k^2]}$$

where n_0 is the index of the substrate and the ambient medium is air (Ref. 7).

Values of k calculated by this method are shown in Figs. 6-13, 6-14, and 6-15 along with slopes calculated from published values of k for silver films. Values for k at 3220 Å and 3600 Å were taken from the work of Huebner et al (Ref. 9) while k at 4000 Å is from Schulz and Tangherlini (Ref. 10).

The absorption index as a function of wavelength obtained from this work is compared in Fig. 6-16 with prior published results on thin silver films and the bulk silver data of Ehrenreich and Philipp (Ref. 11). Agreement with the prior thin film data is fairly good at 3220 Å and 4000 Å but is considerably lower at intermediate wavelengths. This discrepancy is very likely due to the fact that the silver films in this work were not well annealed and may have been somewhat optically inhomogeneous.

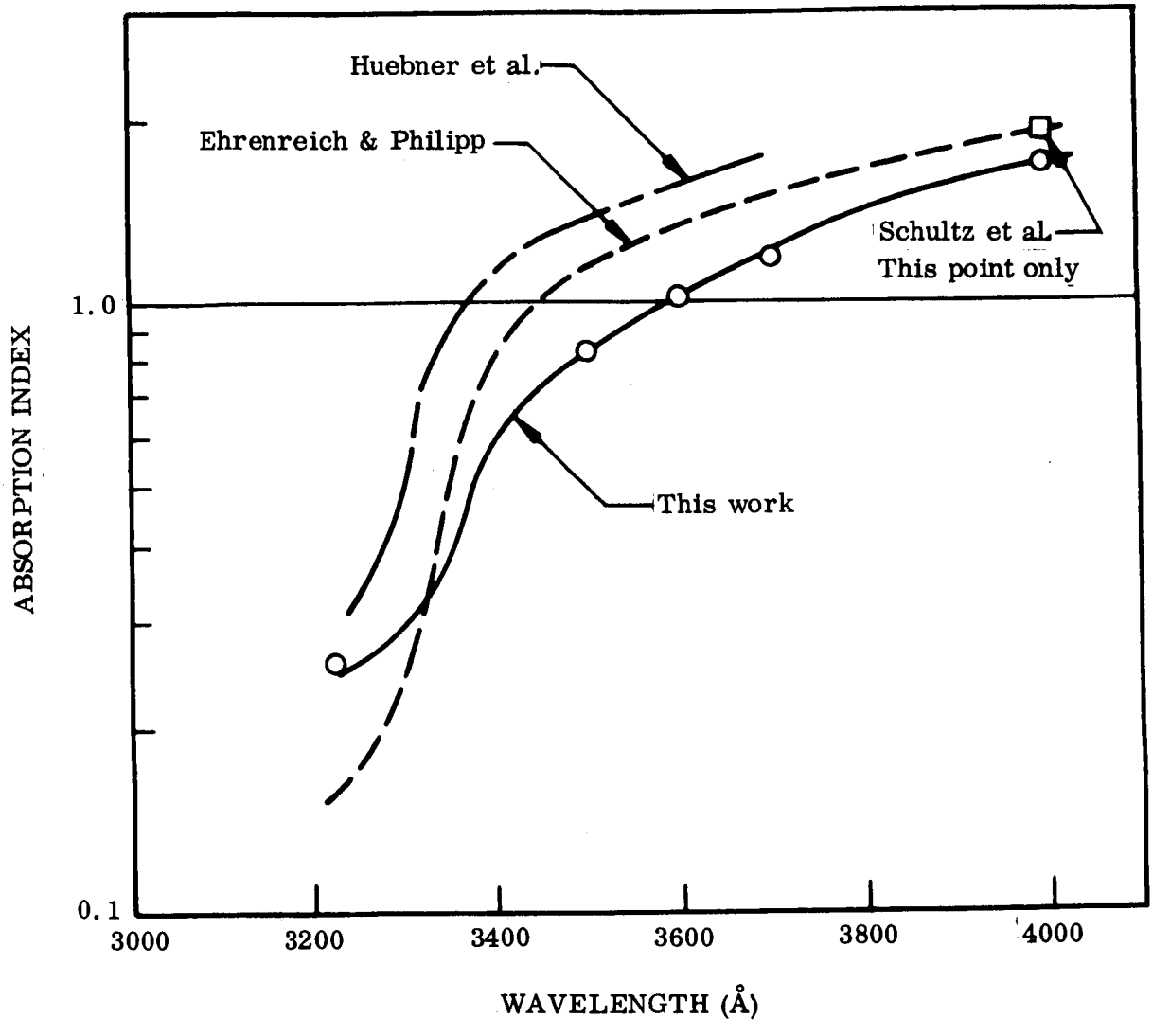

Fig. 6-16 Absorption Index of Silver as a Function of Wavelength

6.7 TRANSMITTANCE OF ALUMINA FILMS

In order to perform analytical studies of the directional reflectance properties of the alumina/silver system, it was necessary to determine the absorption coefficient of the deposited Al_2O_3 films as a function of wavelength.

Films of Al_2O_3 were deposited on NaCl flats. Al_2O_3 films of 1080, 2500, 5000, and 10,000 Å thicknesses were prepared at a deposition rate of 10 to 15 Å/sec. The spectral transmittance of each film thickness was measured over the wavelength range 1.5 to 14.5 μ. In addition, a 0.032 in. thick sapphire plate was measured, in order to estimate the absorption coefficient in the near infrared region. Spectral transmittance plots are shown in Fig. 6-17.

The spectral transmittance for the electron beam deposited aluminum oxide films is essentially identical in character with anodized Al_2O_3 films of equivalent thickness. (Ref. 12). The absorption band at 11 μ observed for Al_2O_3 on silver is absent for the films deposited on NaCl.

The monochromatic transmittance of Al_2O_3 films as a function of film thickness is shown in Fig. 6-18. Values of absorption index (k) and absorption coefficient ($\alpha = 4\pi k/\lambda$) calculated from these data are also shown in Fig. 6-18. At 5 μ the value of k obtained from the sapphire sample was found to be approximately 4×10^{-4}. At longer wavelengths k was found to increase to a maximum value of 1.65 near 14 μ.

The values of absorption index obtained in this study were generally 30 to 50% higher than those reported by Harris (Ref. 12) for anodized films. This difference can be attributed to difference in thickness measurement techniques for evaporated and anodized films, as well as to the fact that refractive index effects were not considered in the calculation of k in this work.

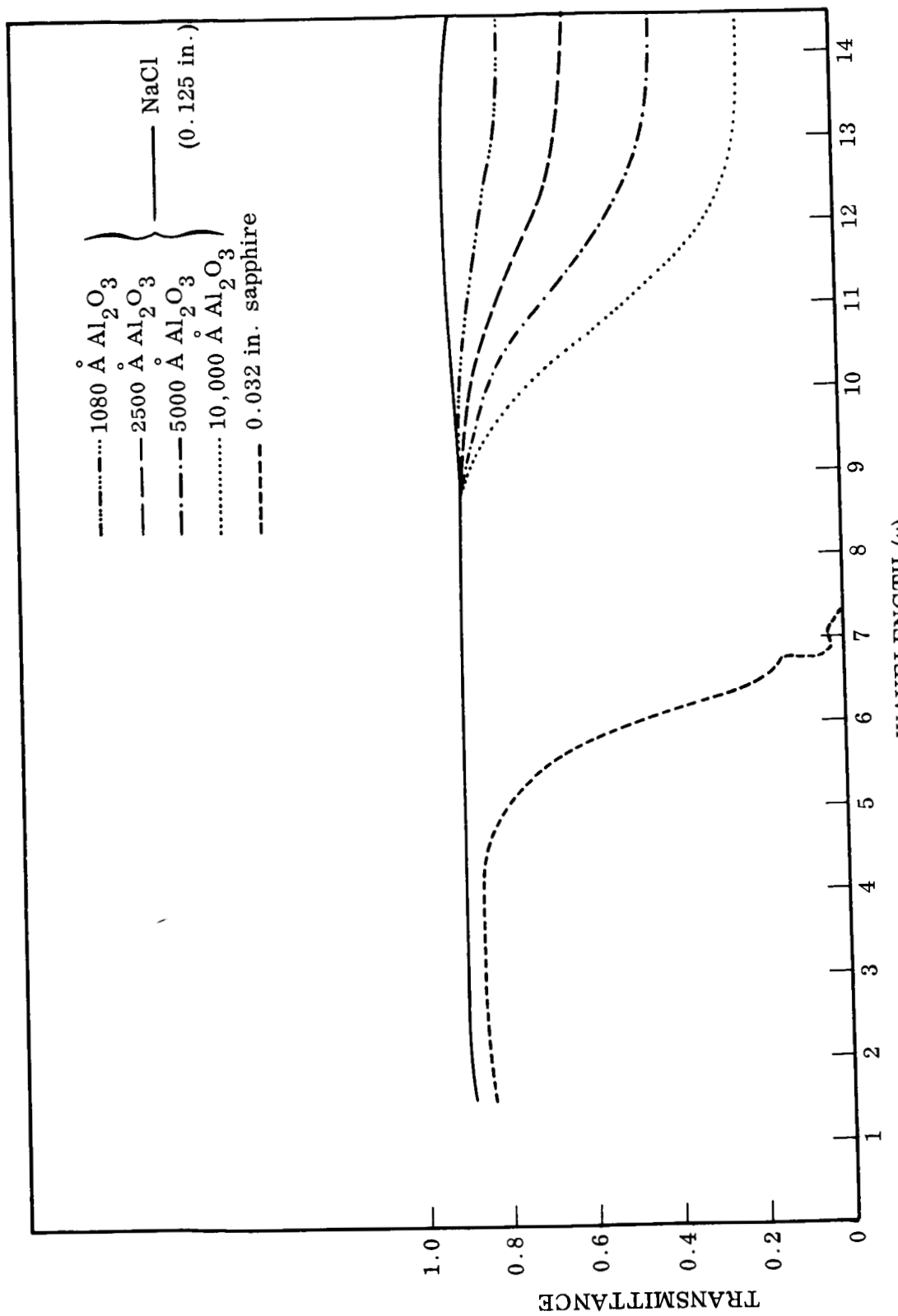

Fig. 6-17 Spectral Transmittance of Aluminum Oxide

A comparison of results of anodized and evaporated aluminum oxide films is as follows:

Film Thickness (μ)	Anodized Film (k) (Ref. 12)	Evaporated Film (k)
5	0.00	4×10^{-4}*
10	0.10	0.17
11	0.36	0.51
12	0.66	1.08
14	1.26	1.65

*0.032 in. Thick Sapphire flat

At wavelengths beyond 10 μ, the absorption coefficients for the alumina films are very large, so that it is to be expected that Al_2O_3 thicknesses of the order of 1000 Å will have marked effects upon both the normal and directional emittance of silver films.

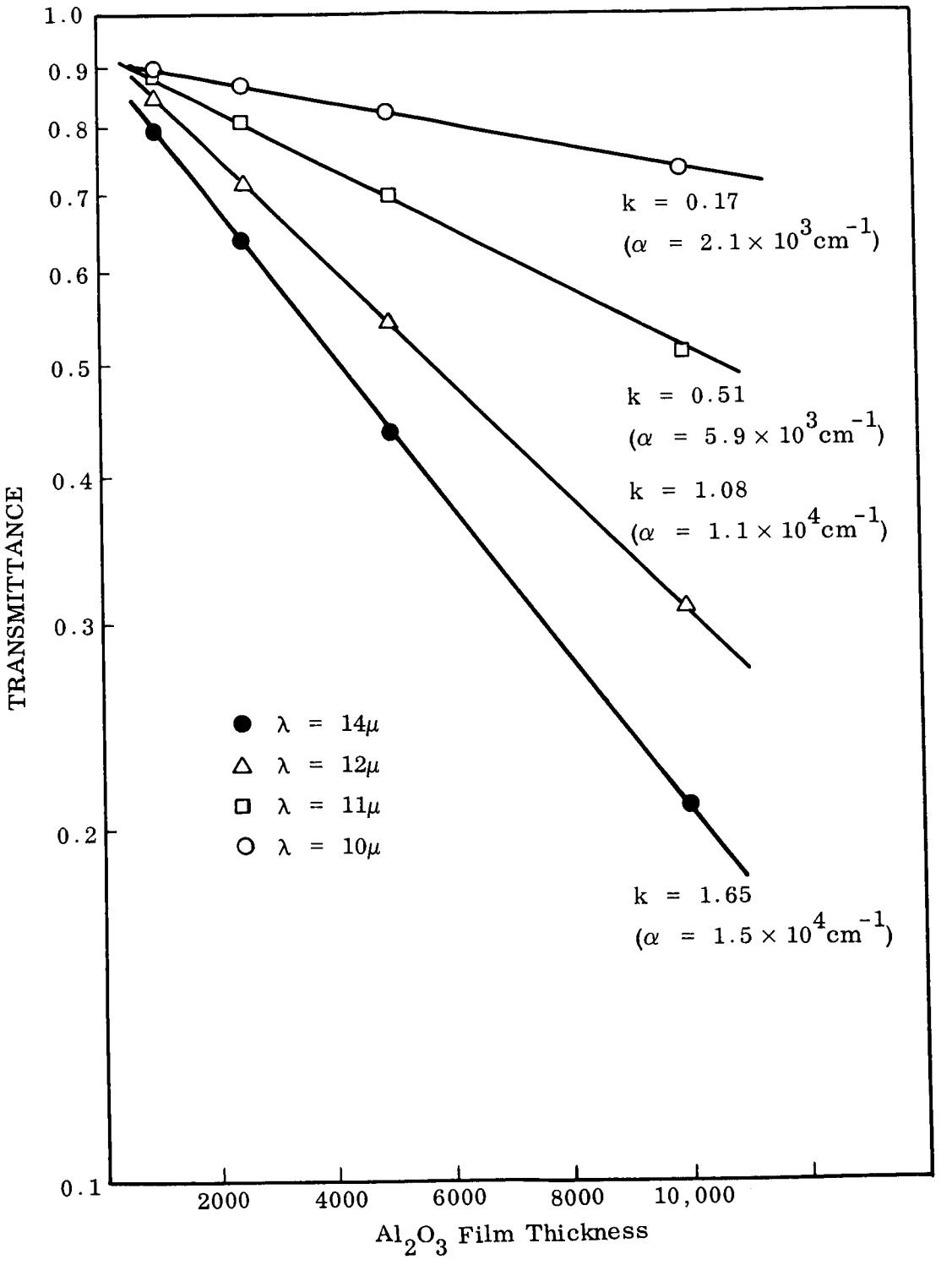

Fig. 6-18 Infrared Absorption Coefficients of Al_2O_3 Films

Section 7
DISCUSSION

7.1 TRANSMITTANCE OF SILVER FILMS

The results obtained with silver films on silica and sapphire substrates are consistent with the above expression. The transmittance is observed to be an exponential function of the film thickness, for silver films thicker than approximately 500 Å. In addition, as predicted by the expression, the absolute value if transmittance depends upon the refractive index of the substrate, the larger the index the lower the transmittance. For Mylar substrates, the situation is more complex due to the finite value of the absorption index. In the spectral region where k for Mylar is very small, the transmittance relationship to silver film thickness approximates that of the other substrates.

For a particular substrate, it is possible to monitor the film thickness by optical transmittance methods. This procedure can yield accurate thickness measurements if appropriate calibration curves are constructed and the films are optically homogeneous. For silver films, the transmission window at 3220 Å provides a convenient point for such measurements. Large values of transmittance are obtained even with films thicker than 1000 Å, thereby increasing the inherent accuracy of measurement.

The effect of deposition rate on the optical properties of silver films was investigated. Silver deposition rates in the range 20 to 200 Å/sec appeared to have little or no effect upon the optical properties of the films. However, the partial pressure of oxygen in the chamber during evaporation influences both reflectance and transmittance. The effect is most pronounced on n, the real part of the index, which is a measure of the free electron concentration in the metal. In addition, the effect of substrate temperature is important, in influencing silver recrystallization and film homogeneity.

7.2 EMITTANCE RELATIONSHIPS

The values of normal emittance (ϵ_N) and total hemispherical emittance (ϵ_H) for bare silver films have been reported to be 0.01 and 0.013, respectively (Ref. 13). The changes in ϵ_N and ϵ_H produced by evaporated overlays of Al_2O_3 on aluminum films have been described by Hass, et al (Ref. 5). In that work, the ratio of ϵ_H/ϵ_N was found to vary with dielectric thickness and to reach values greater than 3 in the vicinity of 2500 Å of Al_2O_3. Similar results have been obtained in this study, on the basis of measurements of directional spectral reflectance and calorimetric hemispherical emittance.

The calorimetric measurements of emittance indicated that ϵ_H is a weak function of temperature for Al_2O_3 thicknesses in the range 245 − 1045 Å. The minimum in the vicinity of 500°K is attributed to the fact that the blackbody curve at the temperature peaks in the spectral region of high constant reflectance for the coating. At 300°K, the absorption band between 10 − 12 μ nearly coincides with the blackbody maximum, thereby raising the emittance. Similarly, the absorption band in the 4 μ region significantly contributes to the emittance at 750°K.

In contrast to the evaporated films, the emittance of the Optical Solar Reflector decreases monotonically with increasing temperature. The emittance decreases from a 300°K value of 0.80 to 0.67 at 750°K.

Comparison of ϵ_H measured calorimetrically with ϵ_N calculated from near normal spectral reflectance yields values of ϵ_H/ϵ_N of approximately 4.5 for the silver films with Al_2O_3 overlays of 245−1045 Å thickness. The ratios ϵ_H/ϵ_N obtained are higher than those reported by Hass (Ref. 3) for Al_2O_3 on Al. The difference appears to be due to the lower measured values of ϵ_N for the silver films.

The calorimetrically determined hemispherical emittance is a linear function of Al_2O_3 thickness at 300 °K. However, at 500 °K, the emittance decreases fairly rapidly at small dielectric thicknesses.

The spectral normal reflectances of the 955 Å, 550 Å, and 210 Å, Al_2O_3 films on silver appear to be very similar to that of bare silver. The major difference is an absorption band centered at 11 μ which is most pronounced for the thickest dielectric film. In addition, the 955 Å Al_2O_3 film shows a slight overall decrease in reflectance compared to the other samples at wavelengths greater than 8 μ, consistent with the high values of absorption coefficient of Al_2O_3 in this spectral region.

The relative spectral directional reflectance $(\rho_{\theta,\lambda}/\rho_{N,\lambda})$ of the Ag/Al_2O_3 samples indicate that for large values of k, for a given value of θ and λ, the emittance increases with Al_2O_3 thickness. However, where the absorption coefficient of the overcoating is small (i.e., at 5 μ) the directional reflectance approaches that of the bare silver.

A rigorous treatment of the directional radiative properties of metal/dielectric layers is given in the Appendix.

A more simplified analysis of directional reflectance properties of metal/dielectric coatings can be made based on the assumption that the effects of refractive index of the dielectric are of second order importance to the absorption index, k.

Considering a ray of monochromatic radiation of intensity to incident at an angle θ to the normal, the intensity at the metal-dielectric interface is given by $I_o \exp^{-4\pi kd/\lambda}$ where d is the dielectric thickness. The intensity is diminished by the reflectance at the metal-dielectric interface and further attenuated by the second pass through the dielectric.

On this basis, the ratio of incident to reflected intensity is given by

$$\frac{I_r^\theta}{I_o} = R_{metal}^\theta \exp^{-8\pi kd/\lambda \cos\theta}$$

where $d/\cos\theta$ is the distance traversed in the dielectric. The ratio of directional to normal reflectance is then given by

$$\frac{I_r^\theta}{I_r^N} \approx \frac{R_m^\theta}{R_m^N} \frac{\exp^{-8\pi kd/\lambda \cos\theta}}{\exp^{-8\pi kd/\lambda}}$$

Since the directional reflectance of silver is nearly constant for angles less than 80° in the infrared, $R_m^\theta/R_m^N \approx 1$ so that the relative directional reflectance can be approximated by

$$\frac{\rho(\theta)}{\rho(N)} \approx \frac{\exp^{-8\pi kd/\lambda \cos\theta}}{\exp^{-8\pi kd/\lambda}}$$

The validity of this approximation is demonstrated by comparison of calculated and measured values of $\rho(\theta)/\rho_N$ at $11\,\mu$, (Table 7-1), using the experimentally determined value of $\alpha_{11\mu} = 5.1 \times 10^3\ cm^{-1}$.

Table 7-1

	θ	20°	40°	60°	70°	75°
d = 955Å Al_2O_3	ρ_θ/ρ_n (calc.)	0.995	0.970	0.905	0.825	0.752
	ρ_θ/ρ_n (measured)	1.00	0.962	0.890	0.825	0.780
d = 550Å Al_2O_3	ρ_θ/ρ_n (calc.)	0.996	0.977	0.942	0.890	0.843
	ρ_θ/ρ_n (measured)	1.00	0.975	0.925	0.880	0.845
d = 210Å Al_2O_3	ρ_θ/ρ_n (calc.)	0.998	0.995	0.980	0.962	0.942
	ρ_θ/ρ_n (measured)	1.00	0.993	0.975	0.955	0.940

It is apparent that the agreement is surprisingly good considering the somewhat drastic approximations inherent in the analysis. For larger thicknesses of dielectric, it is to be expected that this expression will be greatly in error. For the case where energy absorption becomes large, the reflectance of the coating will be dominated by the properties of the dielectric-air interface. Since the front surface reflectance of the system increases with angle of incidence, it is to be expected that $\rho(\theta,\lambda)/\rho(N,\lambda$ will increase implying that $\epsilon(\theta,\lambda)/\epsilon(N,\lambda) < 1$. This case is observed for Al_2O_3 films of thickness greater than 15,000 Å on aluminum (Ref. 5), where $\epsilon_H \approx 0.4$.

It is interesting to note that the hemispherical reflectance or emittance can be approximated by selecting the value at an angle of 55° from normal. This estimate is based on the fact that the average value of cos θ corresponds to approximately 55°. This technique provides for a rapid evaluation of the hemispherical to normal reflectance ratio (or emittance) that requires only two measurements at each wavelength.

Section 8
CONCLUSIONS

8.1 FILM DEPOSITION

There is considerable latitude in the deposition of silver films to obtain a minimum value of solar absorptance. Deposition rates of 20 to 200 Å/sec result in comparable α_s.

In the temperature range of room temperature to 500°K and in the deposition rate range of 20 to 200 Å/sec the optical characteristics remain essentially invariant. Greater variations can be expected from substrate surface quality, inconsistency in substrate cleaning and maintenance of a non-contaminated silver evaporation source.

The problem of silver adhesion can be very satisfactorily solved by a mild hydrofluoric substrate etch followed by substrate heating to the order of 500°K prior to vacuum deposition. No change in α_s results from this surface treatment.

The corrosion resistance of alumina overcoated silver is high. On the basis of a very accelerated test in a highly corrosive hydrogen sulfide atmosphere, the indication is that alumina of a minimum thickness of 500 Å is very acceptable. In a corrosive environment the attack starts at the exposed substrate edge.

8.2 PROTON ENVIRONMENT

The stability of fused silica with an integrated exposure of 5×10^{17} p/cm^2 and substrate temperature to 700°K was excellent. No change in α_s resulted from this exposure regardless of the source or grade of the fused silicas tested.

8.3 OSR ULTRAVIOLET EXPOSURE

Exposure of the OSR's to 500 ESH of ultraviolet at 700°K resulted in the order of 1% change in α_s. This was shown to be due to a change in transmittance of the fused silica.

8.4 SILVER FILM TRANSMITTANCE

The results of the deposition of silver films on SiO_2, Al_2O_3 and Mylar substrates indicate that the transmittance is an exponential function of the silver film thickness greater than 500 Å. The optical properties of the substrate determine the absolute magnitude of the transmittance at a given film thickness. Transmittance measurements are difficult to analyze at wavelengths where the substrate exhibits appreciable absorption.

8.5 EMITTANCE RELATIONSHIPS

The total hemispherical emittance of the Optical Solar Reflector decreases approximately 15% as the temperature increases from 300° to 750°K. Serious errors in emittance measurements for this system can result from failure to accurately measure the front surface temperature.

The total hemispherical emittance of the Ag/Al_2O_3 coating first decreases then in increases as the temperature is varied from 300° to 750°K. The minimum emittance occurs near 500°K. The ratio of hemispherical to normal emittance is approximately 4.5 in the Al_2O_3 thickness range 245° – 1045Å.

Spectral directional reflectance measurements on silver coated with alumina indicate that the emittance increases with both angle of incidence and dielectric layer thickness in the spectral regions where the absorption index of the dielectric is large. Absolute values of emittance are subject to large uncertainties due to the highly reflecting nature of the coating system. Relative spectral directional reflectance can be calculated by a simple model for dielectric thicknesses less than 1000 Å, if the optical properties of the material are known.

Section 9

REFERENCES

1. Final Report, Low Solar Absorptance and Emittance Surfaces Utilizing Vacuum Deposited Techniques, Report No. CR-73039, Contract No. NAS 2-3063, Oct 1966
2. O. S. Heavens, "Optical Constants of Thin Films," in Physics of Thin Films, Vol. 2, ed. by G. Hass and R. E. Thun, Academic Press, N. Y., 1964
3. J. E. Francis and T. J. Love, "Radiant Heat Transfer of Isothermal Diathermanous Coatings on a Conductor," AIAA J. 4 (1966)
4. O. J. Edwards, Optical Transmittance of Fused Silica at Elevated Temperatures, J. Opt. Soc. 56, No. 10, Oct 1966
5. ASTM/IES/AIAA, Second Simulation Conference, American Society for Testing and Materials, 1967
6. R. V. Dunkle et al., "Heated Cavity Reflectometer for Angular Reflectance Measurements," in Progress in International Research on Thermo. and Transport Prop., Am. Soc. Mech. Engrs., New York, Academic Press, 1962, p. 541
7. G. Hass, "Optical Properties of Metals," in AIP Handbook, 2nd Ed., pp. 6−103
8. G. Hass et al., "Solar Abosrptance and Thermal Emittance of Aluminum Coated With Surface Films of Evaporated Aluminum Oxide," in AIAA Progress in Astronautics and Aeronautics, Vol. 18, ed. by G. B. Heller, Academic Press, N. Y., 1966
9. R. H. Huebner, E. T. Arakawa, R. A. MacRae, and R. N. Hamm, "Optical Constants of Vacuum-Evaporated Silver Films," J. Opt. Soc. Am., 54, 1434 (1964)
10. L. G. Shulz and F. R. Tangherline, J. Opt. Soc. Am., 44, 362 (1954)
11. H. Ehrenreich and H. R. Phillipp, Phys. Rev. 128, 1622 (1962)

12. L. Harris, "Preparation and Optical Properties of Aluminum Oxide Films, J. Opt. Soc. Am. 45, 27 (1954)

13. L. F. Drummeter and G. Hass, "Solar Absorptance and Thermal Emittance," in Physics of Thin Films, Vol. 2, ed. by G. Hass and R. E. Thun, Academic Press, N.Y., 1964

Appendix

CALCULATION OF REFLECTANCE CURVES OF A METAL WITH A THIN ABSORBING DIELECTRIC FILM

A.1 DERIVATION OF REFLECTANCE

Equation of a Metal with Thin Absorbing Film

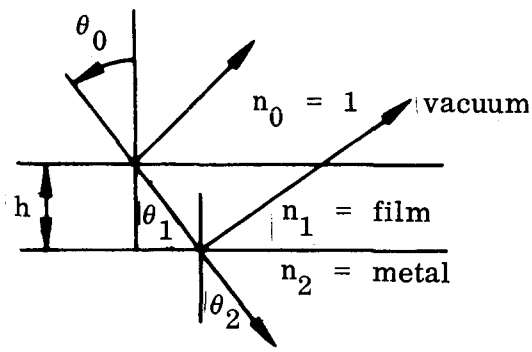

Fig. A-1

Consider a plane wave incident upon a metal coated with a dielectric thin film, the reflection coefficient can be written as (Ref. 1).*

$$r + \frac{r_{01} + r_{12} e^{2i\beta}}{1 + r_{01} r_{12} e^{2i\beta}} \tag{1}$$

where r_{01}, r_{12} are the corresponding coefficients associated with the reflection at the first and second faces respectively. In the case of a slightly absorbing thin film, the quantity

$$\beta = \frac{2\pi}{\lambda_0} \tilde{n}_1 \cos \theta_1$$

is complex because of the complex refractive index

$$\tilde{n} = n + ik$$

where k is the extinction coefficient.

*Appendix References are on p. A-10

In order to calculate the reflectance, we define

$$\left.\begin{aligned} r_{01} &= a + ib \\ r_{12} &= c + id \\ \beta &= \beta_1 + i\beta_2 \end{aligned}\right\} \tag{2}$$

The reflection coefficient given in Eq. (1) can then be rationalized as

$$r = \frac{AC + BD}{C^2 + D^2} + i\,\frac{BC - AD}{C^2 + D^2} \tag{3}$$

where

$$\left.\begin{aligned} A &= a + c\beta_1 - d\beta_2 \\ B &= b + d\beta_1 + c\beta_2 \\ C &= 1 + (ac - bd)\beta_1 - (ad + bc)\beta_2 \\ D &= (ad + bc)\beta_1 + (ac - bd)\beta_2 \end{aligned}\right\} \tag{4}$$

The reflectance can then be calculated from Eq. (3) as

$$\begin{aligned} R(\lambda, \theta_0, h) &= |r|^2 \\ &= \frac{r_{01}^2 + r_{12}^2 \exp(-4\beta_2 h) + 2\exp(-2\beta_2 h)\,\{(ac+bd)\cos 2\beta_1 h + (bc-ad)\sin 2\beta_1 h\}}{1 + r_{01}^2 r_{12}^2 \exp(-4\beta_2 h) + 2\exp(-2\beta_2 h)\,\{(ac-bd)\cos 2\beta_1 h - (bc+ad)\sin 2\beta_1 h\}} \end{aligned} \tag{5}$$

where

$$\left.\begin{aligned} \beta_1 &= \frac{2\pi}{\lambda_0} n_1 \cos\theta_1 \\ \beta_2 &= \frac{2\pi}{\lambda_0} k_1 \cos\theta_1 \end{aligned}\right\}$$

In order to calculate $R(\lambda, \theta_0, h)$ from Eq. (5), we need to calculate a, b, c, d, β_1 and β_2 for a given wave length λ, incident angle θ_0 and film thickness h of the dielectric film on a metal.

The real and imaginary parts of the quantities given in Eq. (2) can be determined as follows. For the first surface between the vacuum and the absorbing thin film, the reflection coefficient, when the electric field is polarized perpendicular to the plane of incidence, is given by (Ref. 2)

$$r_{01}^{TE} = \frac{\cos\theta_0 - (n_1 + ik_1)\cos\theta_1}{\cos\theta_0 + (n_1 + ik_1)\cos\theta_1} = a + ib \tag{7}$$

where

$$\left.\begin{aligned} a &= \frac{\cos^2\theta_0 - n_1^2\cos^2\theta_1 - k_1^2\cos^2\theta_1}{(\cos\theta_0 + n_1\cos\theta_1)^2 + k_1^2\cos^2\theta_1} \\ b &= -\frac{2k_1\cos\theta_0\cos\theta_1}{(\cos\theta_0 + n_1\cos\theta_1)^2 + k_1^2\cos^2\theta_1} \end{aligned}\right\} \tag{8}$$

Similarly, when the electric field is polarized parallel to the plane of incidence, we have

$$r_{01}^{TM} = \frac{\hat{n}_1\cos\theta_0 - \cos\theta_1}{\hat{n}_1\cos\theta_0 + \cos\theta_1} = a' + ib' \tag{9}$$

where

$$\left.\begin{aligned} a' &= \frac{n_1^2\cos^2\theta_0 - \cos^2\theta_1 + k_1^2\cos^2\theta_0}{(n_1\cos\theta_0 + \cos\theta_1)^2 + k_1^2\cos^2\theta_1} \\ b' &= \frac{2k\cos\theta_0\cos\theta_1}{(n\cos\theta_0 + \cos\theta_1)^2 + k_1^2\cos^2\theta_0} \end{aligned}\right\} \tag{10}$$

For the second surface between the thin film and the metal, the reflection coefficients can be developed as follows:

$$r_{12}^{TE} = \frac{\tilde{n}_1 \cos\theta_1 - \tilde{n}_2 \cos\theta_2}{\tilde{n}_1 \cos\theta_1 + \tilde{n}_2 \cos\theta_2} = c + id \tag{11}$$

where

$$c = \frac{\left(n_1^2 + k_1^2\right)\cos^2\theta_1 - \left(n_2^2 + k_2^2\right)\cos^2\theta_2}{\left(n_1 \cos\theta_1 + n_2 \cos\theta_2\right)^2 + \left(k_1 \cos\theta_1 + k_2 \cos\theta_2\right)^2}$$

$$d = \frac{2(k_1 n_2 - n_1 k_2)\cos\theta_1 \cos\theta_2}{\left(n_1 \cos\theta_1 + n_2 \cos\theta_2\right)^2 + \left(k_1 \cos\theta_1 + k_2 \cos\theta_2\right)^2} \tag{12}$$

and

$$r_{12}^{TM} = \frac{\dfrac{\cos\theta_1}{\tilde{n}_1} - \dfrac{\cos\theta_2}{\tilde{n}_2}}{\dfrac{\cos\theta_1}{\tilde{n}_1} + \dfrac{\cos\theta_2}{\tilde{n}_2}} = c' + c'd' \tag{13}$$

where

$$c' = \frac{\left(n_2^2 + k_2^2\right)\cos^2\theta_1 - \left(n_1^2 + k_1^2\right)\cos^2\theta_2}{\left(n_2 \cos\theta_1 + n_1 \cos\theta_2\right)^2 + \left(k_2 \cos\theta_1 + k_1 \cos\theta_2\right)^2}$$

$$d' = \frac{2(k_1 n_2 - n_1 k_2)\cos\theta_1 \cos\theta_2}{\left(n_2 \cos\theta_1 + n_1 \cos\theta_2\right)^2 + \left(k_2 \cos\theta_1 + k_1 \cos\theta_2\right)^2} \tag{14}$$

The values of n and k are assumed to be given as a function of the solid and the wavelength. However, the angle of refraction will be needed in the calculations of r_{01}, r_{12} as well as β_1 and β_2 in Eq. (6). The values of θ_1 can be calculated as follows (Ref. 3).

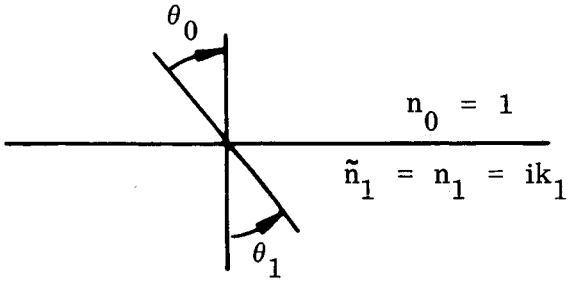

Fig. A-2

If we use the Snell's law of refraction

$$\tilde{n}_1 \sin\theta_1 = n_0 \sin\theta_0$$

and let

$$\tilde{n}_1 \cos\theta_1 = (n_1 + ik_i)\cos\theta = u + iv$$

Then we can obtain

$$\left.\begin{aligned} 2u^2 &= \left(n_1^2 - k_1^2\right) - \sin^2\theta_0 + \left\{\left[\left(n_1^2 - k_1^2\right) - \sin^2\theta_0\right]^2 + 4n_1^2k_1^2\right\}^{1/2} \\ 2v^2 &= \left(n_1^2 - k_1^2\right) - \sin^2\theta_0 + \left\{\left[\left(n_1^2 - k_1^2\right) - \sin^2\theta_0\right]^2 + 4n_1^2k_1^2\right\}^{1/2} \end{aligned}\right\} \quad (15)$$

By the definition of u and v we obtain the expression for the angle of refraction θ_1.

$$2\sin^2\theta_0 = \sin^2\theta_1\left\{\left(n_1^2 - k_1^2\right) + \left[\left(n_1^2 - k_1^2\right)^2 + \frac{4n_1^2k_1^2}{\cos^2\theta_1}\right]^{1/2}\right\} \quad (16)$$

An iteration process is used to obtain θ_1 for Eq. (16).
The value of θ_2 is so small because of the high values of n_2 and k_2 in metals, it can be reasonably assumed that $\theta_2 \cong 0$ for all values of θ_0.

In the case of normal incidence, Eq. (5) becomes identical to the expression derived in Ref. 4.

A.2 APPROXIMATE EQUATION FOR REFLECTANCE CALCULATION

The reflectance can now be calculated from Eq. (5) by use of Eqs. (6) to (16). It can easily be seen that this is a time-consuming, tedious procedure. However, a closer examination of the various terms involved in Eqs. (6) to (16) revealed some valid approximations that can be used to reduce the calculation procedures greatly without sacrificing the accuracy of the results. The values of r_{12} are very close to one. In actual calculation of r_{12} of Al_2O_3 film over silver at $\lambda = 11\mu$, h = 210 Å to 955 Å, we have

$$r_{12}^{TE} \doteq -0.98 + 0.04i$$

$$r_{12}^{TM} \doteq 0.97 + 0.04i$$

The values of the real and imaginary parts do not vary greatly with the incident angle θ_0. Hence, we can assume that

$$\begin{aligned} r_{12}^2 &= 0.96 \\ c &= -c' \doteq -1 \\ d &= d' \doteq 0 \end{aligned} \tag{17}$$

Eq. (5) then becomes

$$R^{TE} = \frac{r_{01}^2 + 0.96 \exp(-4\beta_2 h) - 2\exp(-2\beta_2 h)\left(a' \cos^2 \beta_1 h + b \sin^2 \beta_1 h\right)}{1 + 0.96\, r_{01}^2 \exp(-4\beta_2 h) - 2\exp(-2\beta_2 h)\left(a \cos^2 \beta_1 h - b' \sin^2 \beta_1 h\right)} \tag{18}$$

where

$$r_{01}^2 = a^2 + b^2$$

and

$$R^{TM} = \frac{r_{01}^2 + 0.96 \exp(-4\beta_2 h) + 2 \exp(-2\beta_2 h)\left(a' \cos^2 2\beta_1 h + b' \sin 2\beta_1 h\right)}{1 + 0.96\, r_{01}^2 \exp(-4\beta_2 h) + 2 \exp(-2\beta_2 h)\left(a' \cos^2 2\beta_1 h - b' \sin 2\beta_1 h\right)} \quad (19)$$

where

$$r_{01}^2 = a'^2 + b'^2$$

The values of a, b, a' and b' and calculated from Eqs. (8) and (10).

Since thermal radiation is unpolarized, Eqs. (18) and (19) can be combined in the form (Ref. 5)

$$R = 1/2\,(R^{TE} + R^{TM}) \quad (20)$$

A.3 COMPARISON OF APPROXIMATE EQUATIONS OF REFLECTANCE WITH EXPERIMENTAL DATA

The absolute values of spectral directional reflectance of thin Al_2O_3 film on silver at a wave length of 11μ and temperature of 300°K have been calculated by use of Eqs. (18) and (19). The results are plotted in Fig. A-3 and compared with measured values. In order to make the comparison valid, the experimentally measured values of relative directional reflectance were normalized to the calculated values at $\theta = 0^\circ$. In this manner, the calculated and experimental reflectances were set equal at normal incidence, and the absolute value of reflectance was determined by multiplying the relative directional reflectance at each angle by the calculated normal reflectance.

As shown in Fig. A-3 the calculated and experimental values of direction reflectance agree fairly well for Al_2O_3 films of 550 Å and 955 Å thicknesses. It should be noted

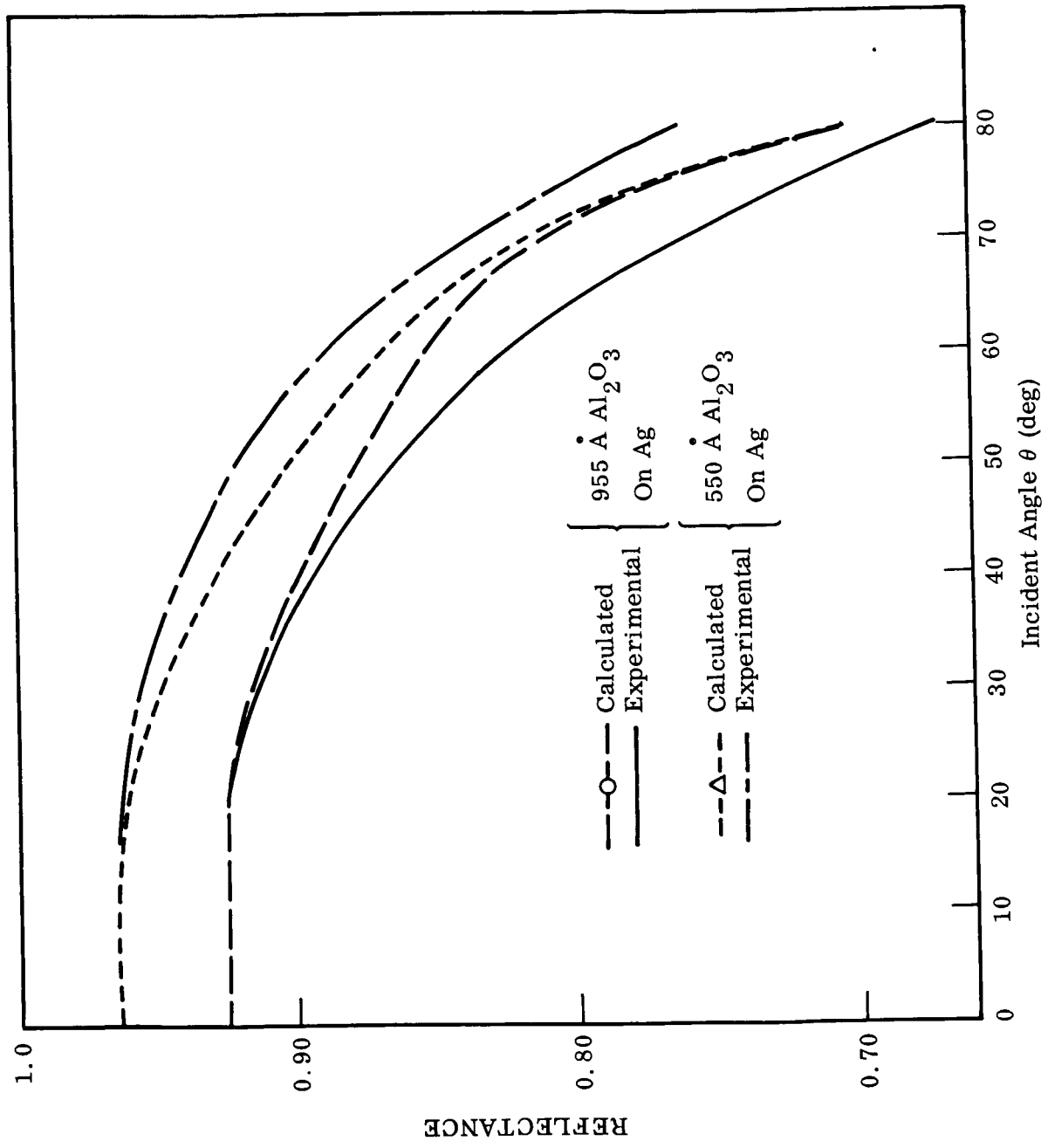

Fig. A-3. Comparison of Calculated and Experimental Directional Reflectance at 11 μ for Alumina on Silver

that the calculated reflectance at $\theta = 80°$ appears to be independent of Al_2O_3 thickness. This may be due to the fact that at grazing angles of incidence, the first surface reflectance predominates over absorption in the coating, and this reflectance is dependent only on the complex index of the dielectric and not the film thickness. The slight discrepancy in this regard between the experimental and calculated values of reflectance may be due to a microscopic surface roughness of the film.

From this analysis, it appears that Eqs. (18) to (20) can be used reliably to predict the directional dependence of reflectance and emittance for metal films with thin dielectric overlays.

REFERENCES

1. M. Born, and E. Wolf., Principles of Optics, Pergamon Press, New York, 1959. pp. 60–61.
2. M. Born, and E. Wolf., op. cit., pp. 625–626.
3. M. Born, and E. Wolf., loc. cit.
4. O.S. Heavens, "Optical Constants of Thin Films," Physics of Thin Films, Vol. 2., G. Hass, and R. F. Thun, eds., Academic Press, New York, 1964. p. 209, Eq. (53).
5. F. Stern, "Elementary Theory of the Optical Properties of Solids," Solid State Physics, Vol. 15, F. Seitz, and D. Turnbull, eds., Academic Press, New York, New York, 1963, p. 320.